Josephson and non-Josephson emission from $Bi_2Sr_2CaCu_2O_{8+\delta}$ mesa structures

Vladimir Krasnov

Experimental Condensed Matter Physics Group
Condensed Matter and Quantum Optics Division
Department of Physics
Stockholm University
AlbaNova University Center
SE-10691 Stockholm, Sweden

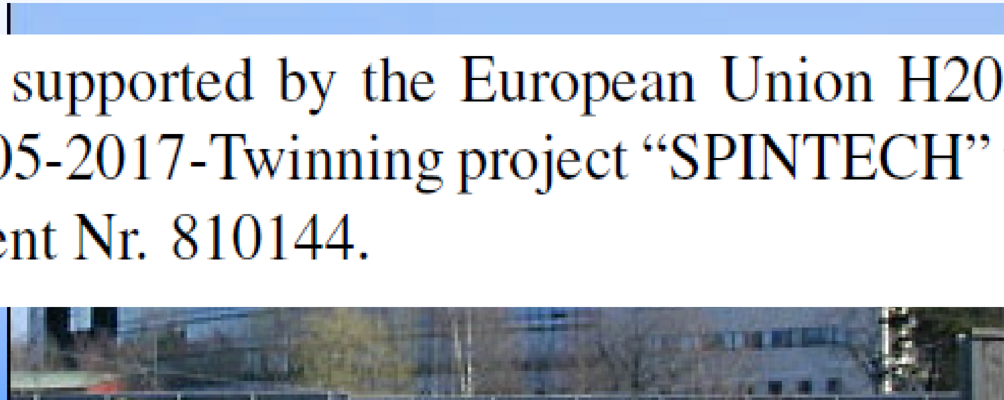

The work was supported by the European Union H2020-WIDESPREAD-05-2017-Twinning project "SPINTECH" under grant agreement Nr. 810144.

P.L. Kapitza Institute of Physical Problems, Moscow, 22 November 2018

The THz gap

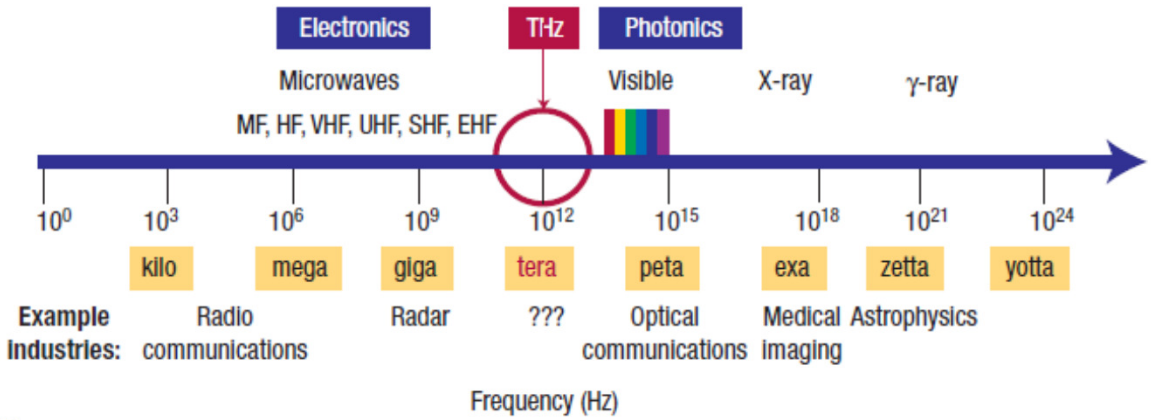

From:
B.Ferguson
and X.C.Zhang
Nature Mat. 1,
26 (2002)

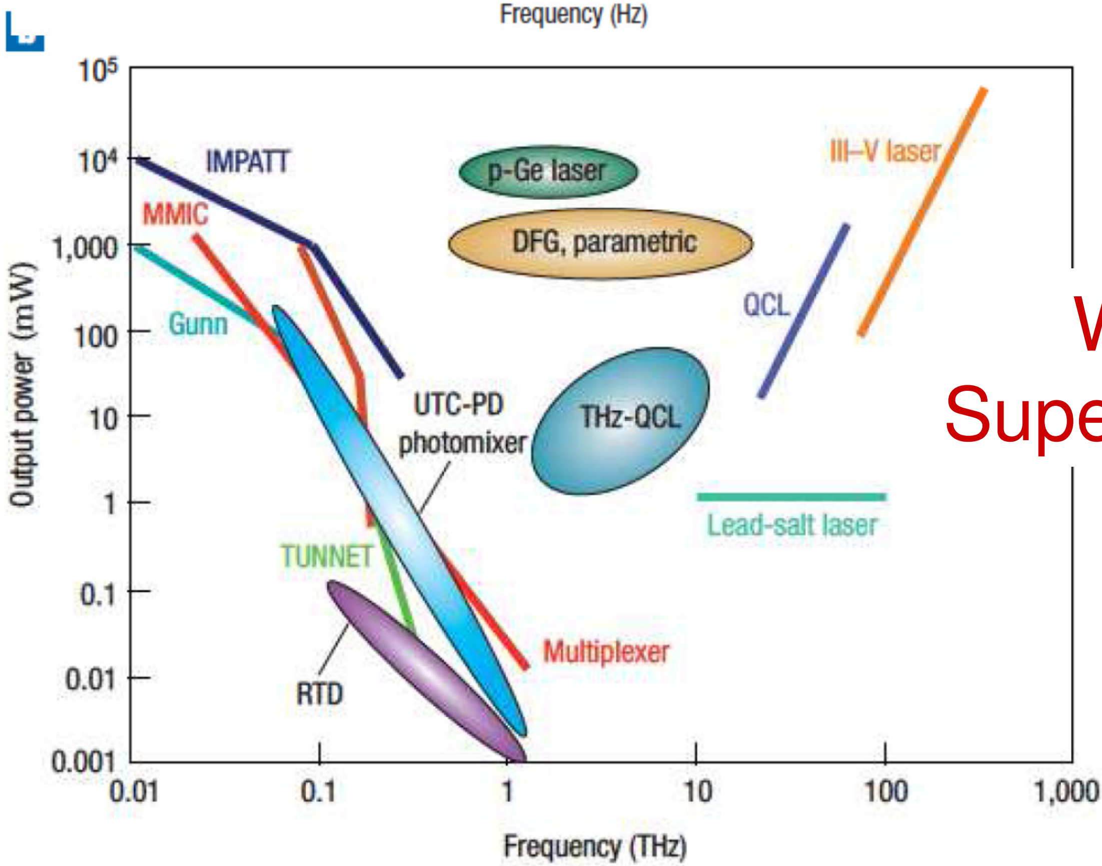

Where are Superconductors ?

From:
M.Tonouchi
Nature Photon.
1, 97 (2007)

Outline:

I. Josephson emission of EM waves:

- Emission via the ac-Josephson effect : $h\nu = 2eV$
- Flux-flow oscillator
- Geometrical (Fiske) resonances

Stacked Josephson junctions

- Coherent superradiant ac-Josephson emission
- Zero-field emission via breather type self-oscillations

II. Semi-Josephson emission :

Monochromatic phonon and phonon-polariton emission via the piezoelectric effect

III. Non-Josephson emission of non-equilibrium bosons: Superconducting cascade laser

Conclusions

I. Josephson emission: ac-J.E. + more

The dc - Josephson effect $\boxed{I_S = I_c \sin(\varphi)}$

The ac - Josephson effect $\boxed{\hbar\,\omega_J = 2eV}$

I. Josephson junctions can generate EM-waves / Photons

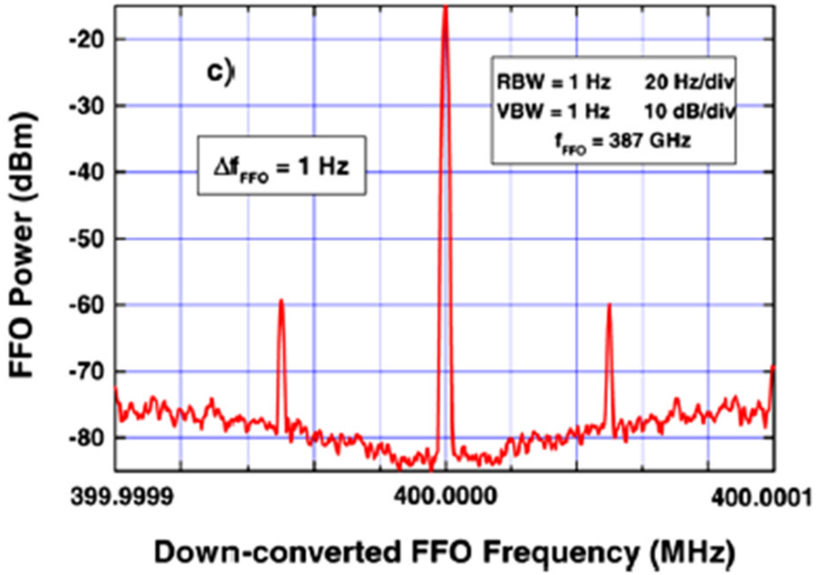

Low-Tc Josephson flux-flow oscillator phase locked to an external reference oscillator

V. P. Koshelets and S. V. Shitov, Supercond. Sci. Technol. **13**, R53 2000.

But the devil is in the details: Supercurrent is non-dissipative need not only dc voltage to ac-(super)current conversion, but dc-to-ac POWER conversion

EM-wave emission by a single junction

$$S = [E_{ac} H_{ac}]$$

$$\nabla \varphi = \frac{2\pi d}{\Phi_0} H$$

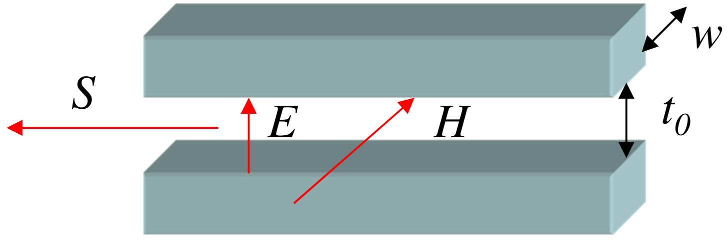

VK, PRB 82, 134524 (2010)

Magnetic field or spatially inhomogeneous phase are needed for dc-to-ac POWER conversion

Need a Lorentz force = finite B!

$$\boxed{F_L = sI \times B}$$

Flux-flow oscillator

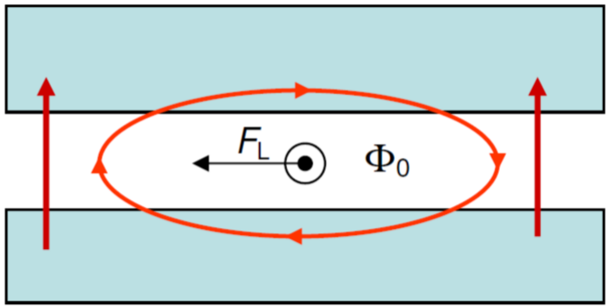

Problem with radiative Impedance matching (outside the JJ):

$$Z = E_{ac} / H_{ac} \quad ??? \sim \sqrt{\mu_0 / \varepsilon_0} = 119.917\Omega$$

Bulaevskii, Koshelev, PRL (2006)

Radiation power: $P_{rad} = w t_0 E_{ac} H_{ac} = w t_0 E_{ac}^2 / Z$ Langenberg etal, PRL 15, 294 (1965)

+ self-heating limitations = low emission power ~ μW

+ Energy storage in relativistic fluxons

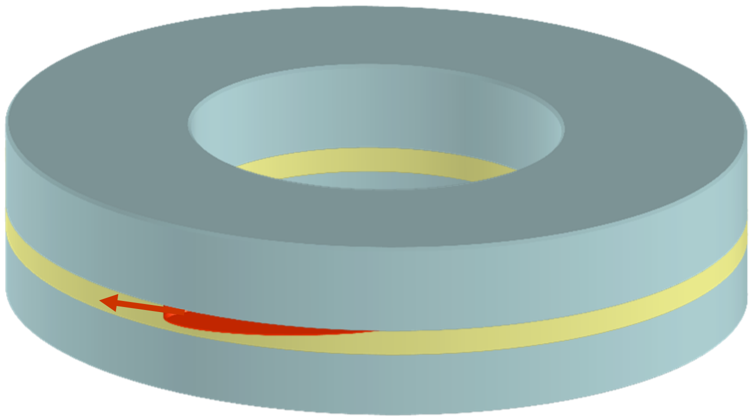

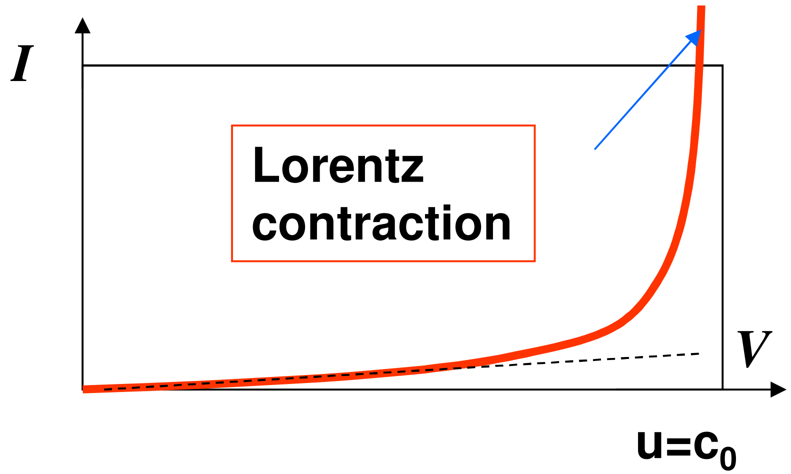

Zero field steps in linear junctions

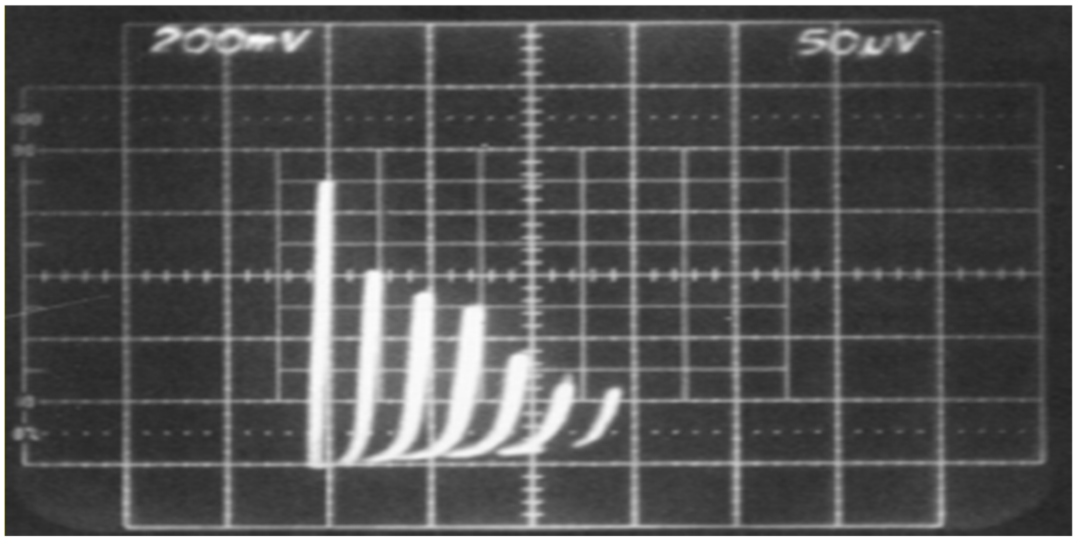

$$V_{ZFS} = \frac{c_0 \Phi_0}{cL} n$$

$V_{ZFS} = 2V_{FS}$

From: A. Barone and G. Paterno

Geometrical resonances: Impedance mismatching is not totally bad

A. High-Q resonances enhance the emission power: $P_{rad} \sim Q^2$

B. High-Q resonances reduce the linewidth: $\Delta f / f = 1/Q$

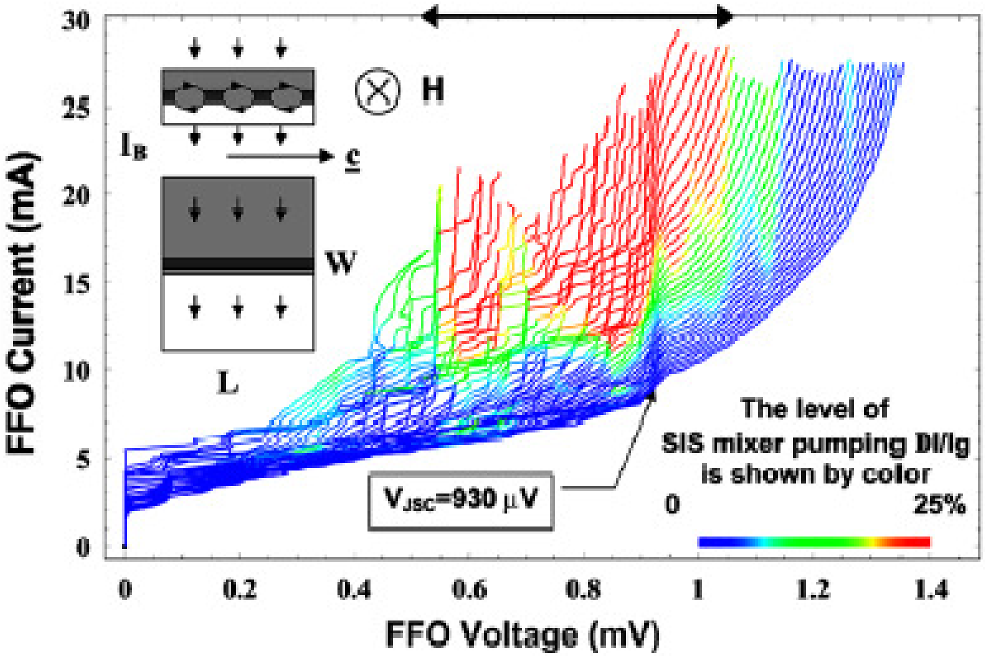

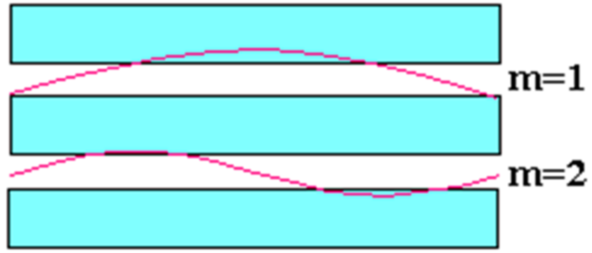

V. P. Koshelets and S. V. Shitov, Supercond. Sci. Technol. **13**, R53 2000.

Flux-flow emission is a 3-step process:

1. Lorentz force accelerates fluxons to the speed of light and store energy.
2. Upon collision with the edge the fluxon energy is given to EM waves.
3. Waves at the cavity mode resonance are amplified, leading to emission.

Where is the ac-J.E. here?

Coherent EM emission from STACKED Josephson junctions

Radiation power:

$$P_{rad} = wt_0 H_{ac} \sum_{i=1}^{N} E_i$$

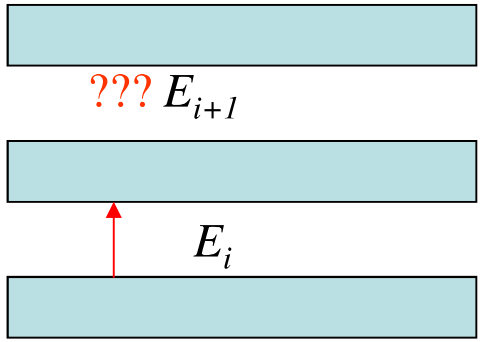

Outside the stack (far field):

$$Z = E_{ac} / H_{ac} \qquad E_{ac} = \sum_{i=1}^{N} E_i$$

VK, PRB 82, 134524 (2010)

$$\boxed{P_{rad} = wt_0 H_{ac} \sum_{i=1}^{N} E_i = wt_0 E_{ac}^2 / Z.}$$

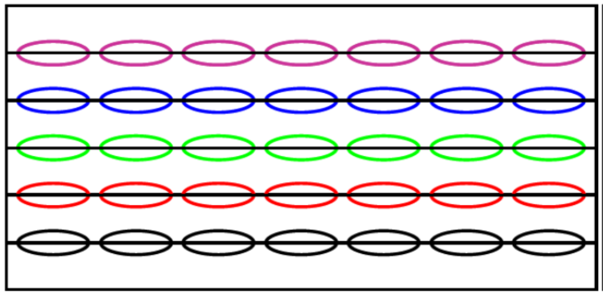

In-phase state: $E_i = E_{i+1}$, $E_{ac} = NE_i$, $\boldsymbol{P \sim N^2}$

Coherent amplification of radiation ☺

Out-of-phase state: $E_i = - E_{i+1}$, $E_{ac} = 0$, $P \sim 0$

Coherent suppression of radiation ☹

2D - cavity modes in stacked Josephson junctions

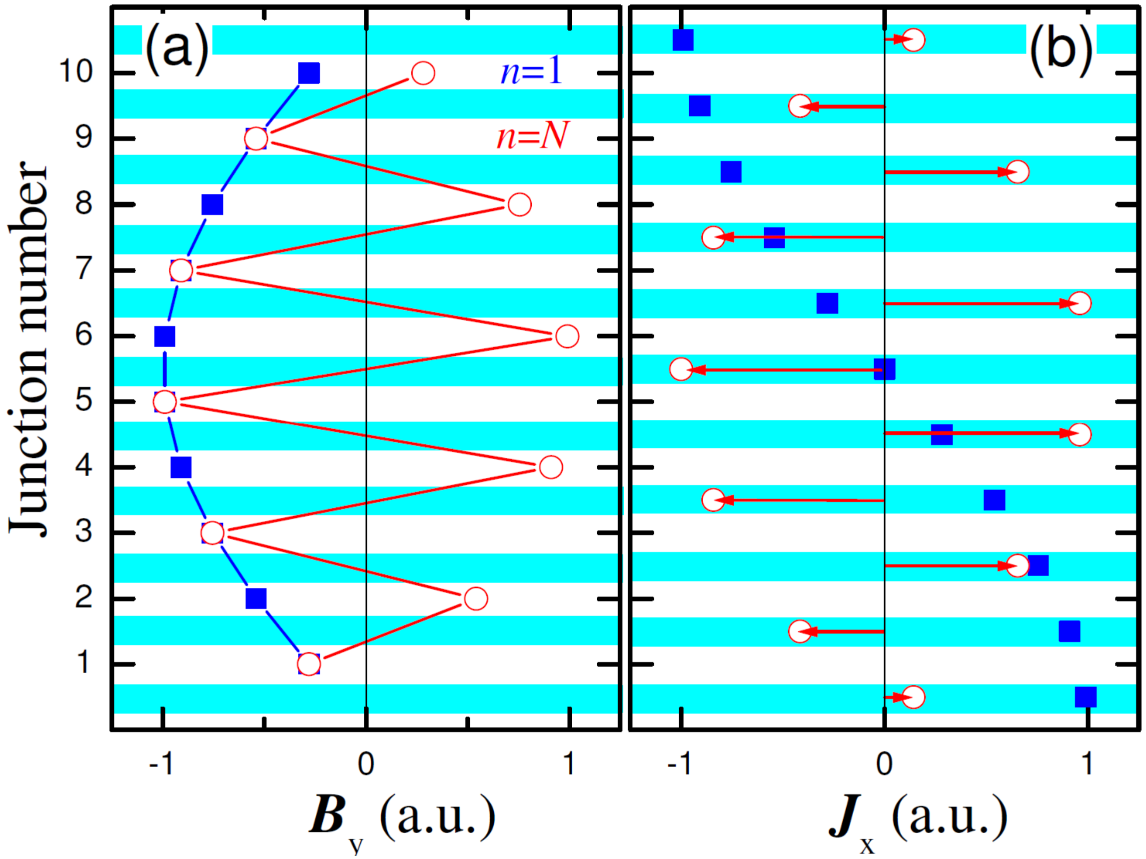

E.N. Economou, Phys.Rev. 182, 539 (1969)

R.Kleiner, Phys.Rev.B 50, 6919 (1994)

S.Sakai, A.V.Ustinov, H. Kohlstedt, A.Petraglia, N.F. Pedersen, Phys.Rev.B 50, 12905 (1994)

$$B_y(x,z)(m,n) = -\frac{H_0 a \pi m \lambda_n^2}{2L\lambda_J} \sin(k_m x) \sin(k_n z)$$

S.O. Katterwe and VK, PRB 84, 214519 (2011)

Intrinsic STACKED Josephson junctions in strongly anisotropic HTSC

$Bi_2Sr_2CaCu_2O_{8+x}$ (Bi-2212)

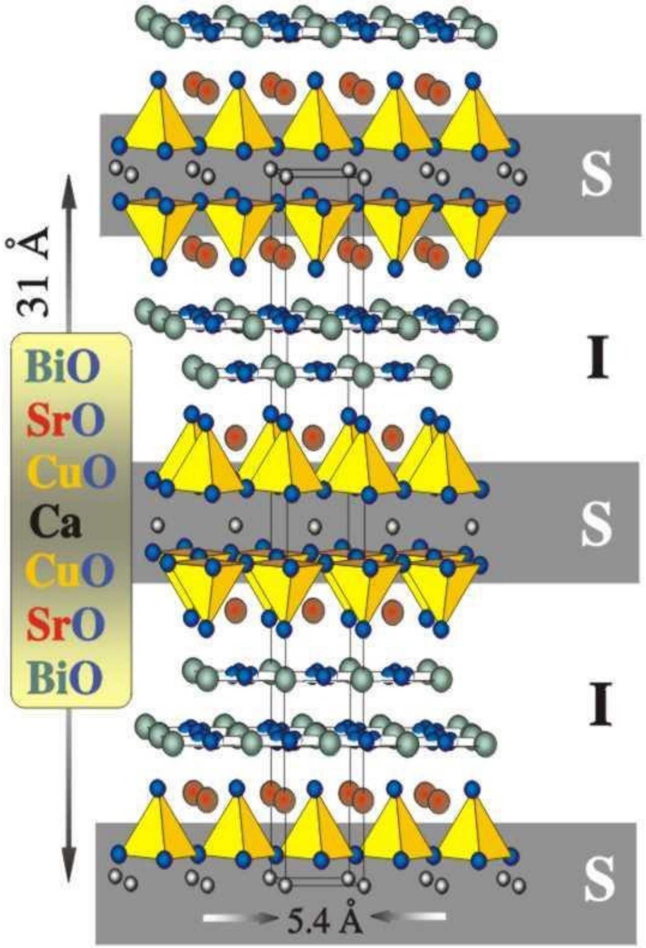

Courtesy of A.Yurgens

c-axis

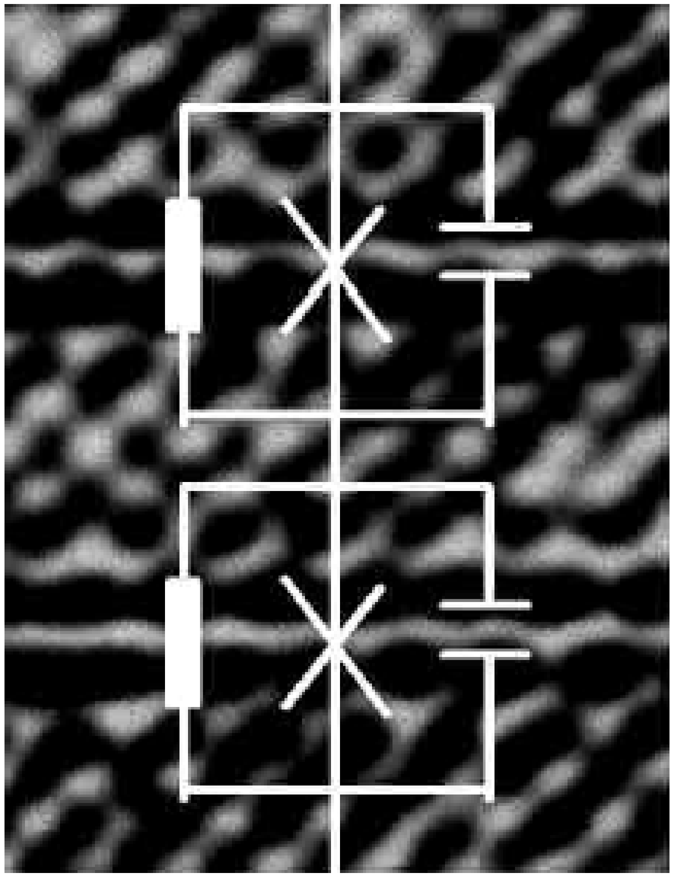

From presentation of P.Mueller

~700 stacked junctions per μm of crystal

Intrinsic Tunneling Characteristics of small Bi-2212 mesas

Advantages of High-Tc intrinsic Josephson junctions:

* High $T_c \approx$ 95K: allows high power

* High Δ~30-40 meV: allows operation up to 20 THz

* Integration of a large amount of strongly coupled junction ~700/mm of a crystal: coherent high power superradiation emission *$P \sim N^2$*

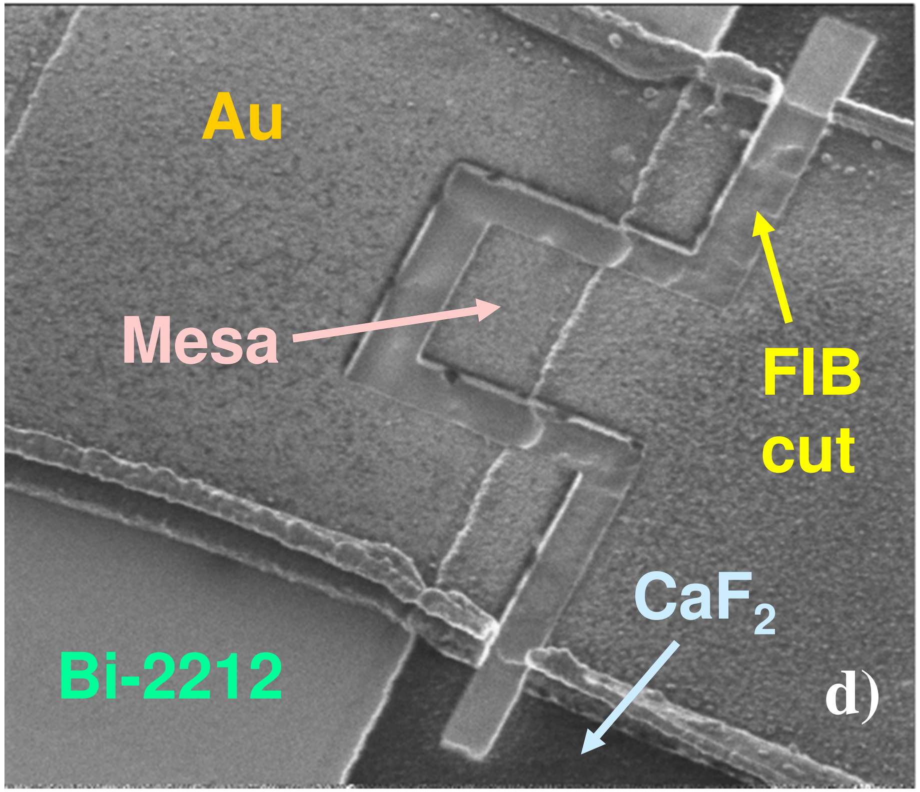

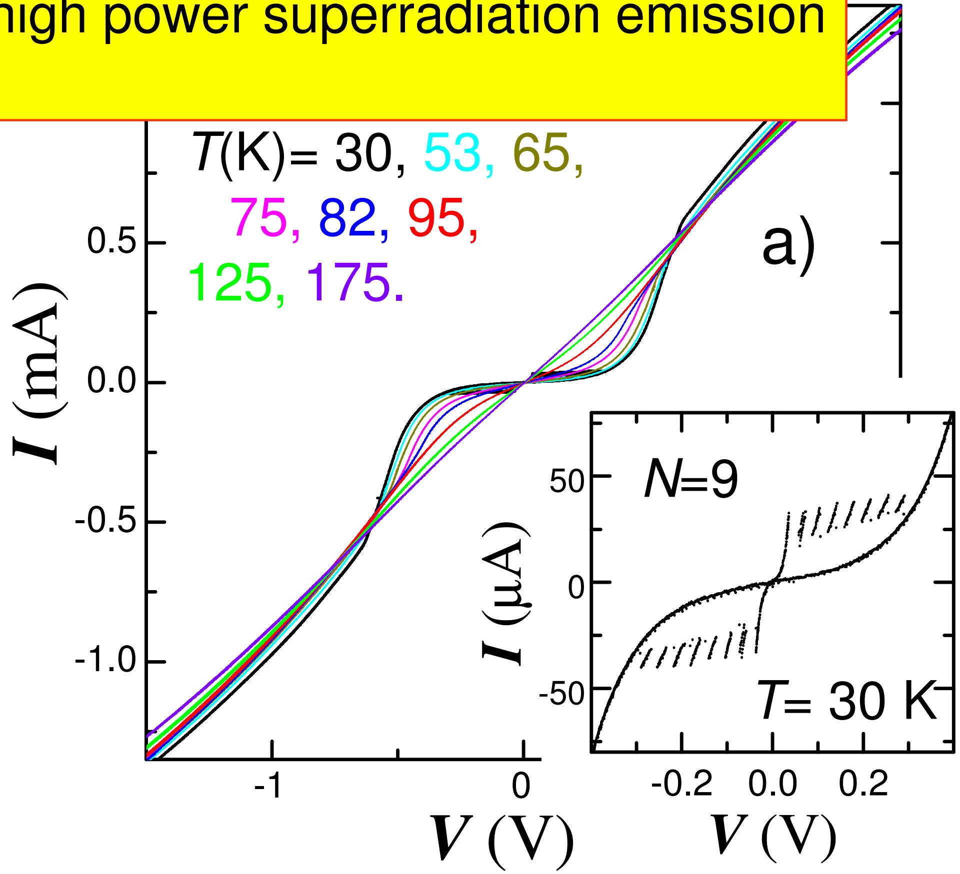

S.O.Katterwe et al, PRL 101, 087003 (2008)

Zero-field EM-wave emission from $Bi_2Sr_2CaCu_2O_{8+x}$ mesa structures

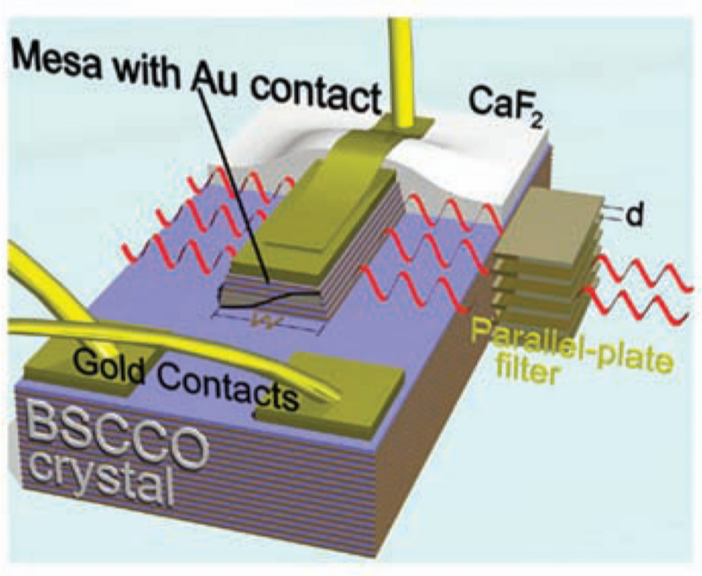

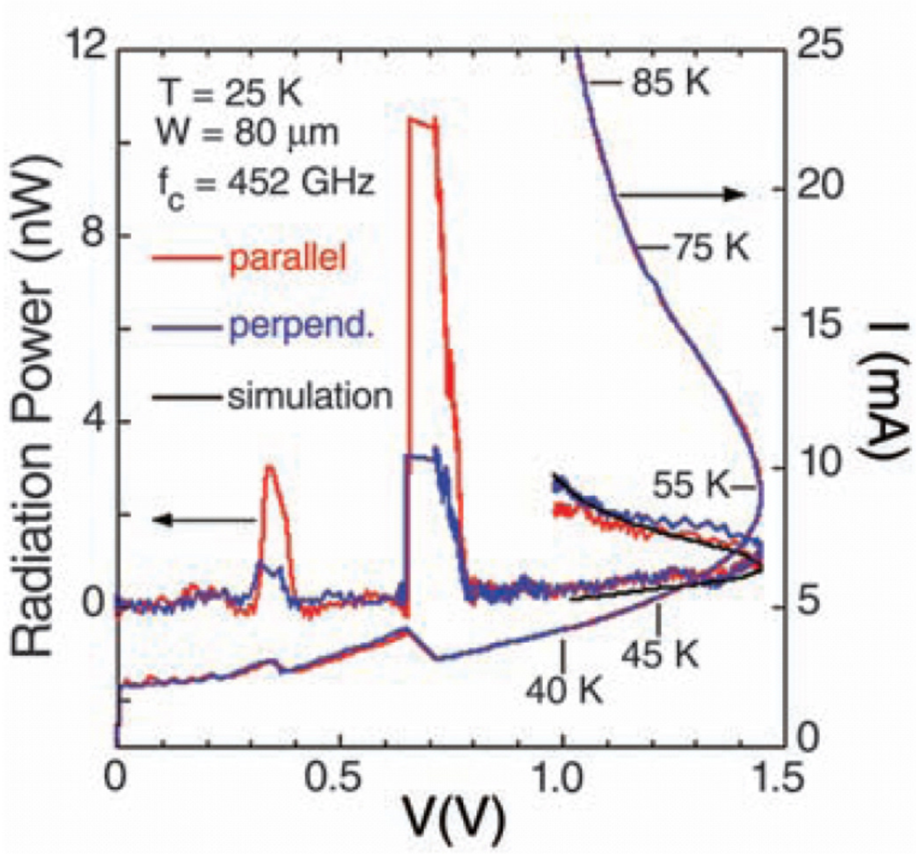

L. Ozyuzer et al, Science **318**, 1291 (2007)

Emission at H=0,
Follows ac- Josephson relation
Scales as f~1/w – geometrical resonance
Superradiant: P~N^2

Mechanism of emission at H = 0 ??? (No Lorentz force)

Standing waves (cavity modes)

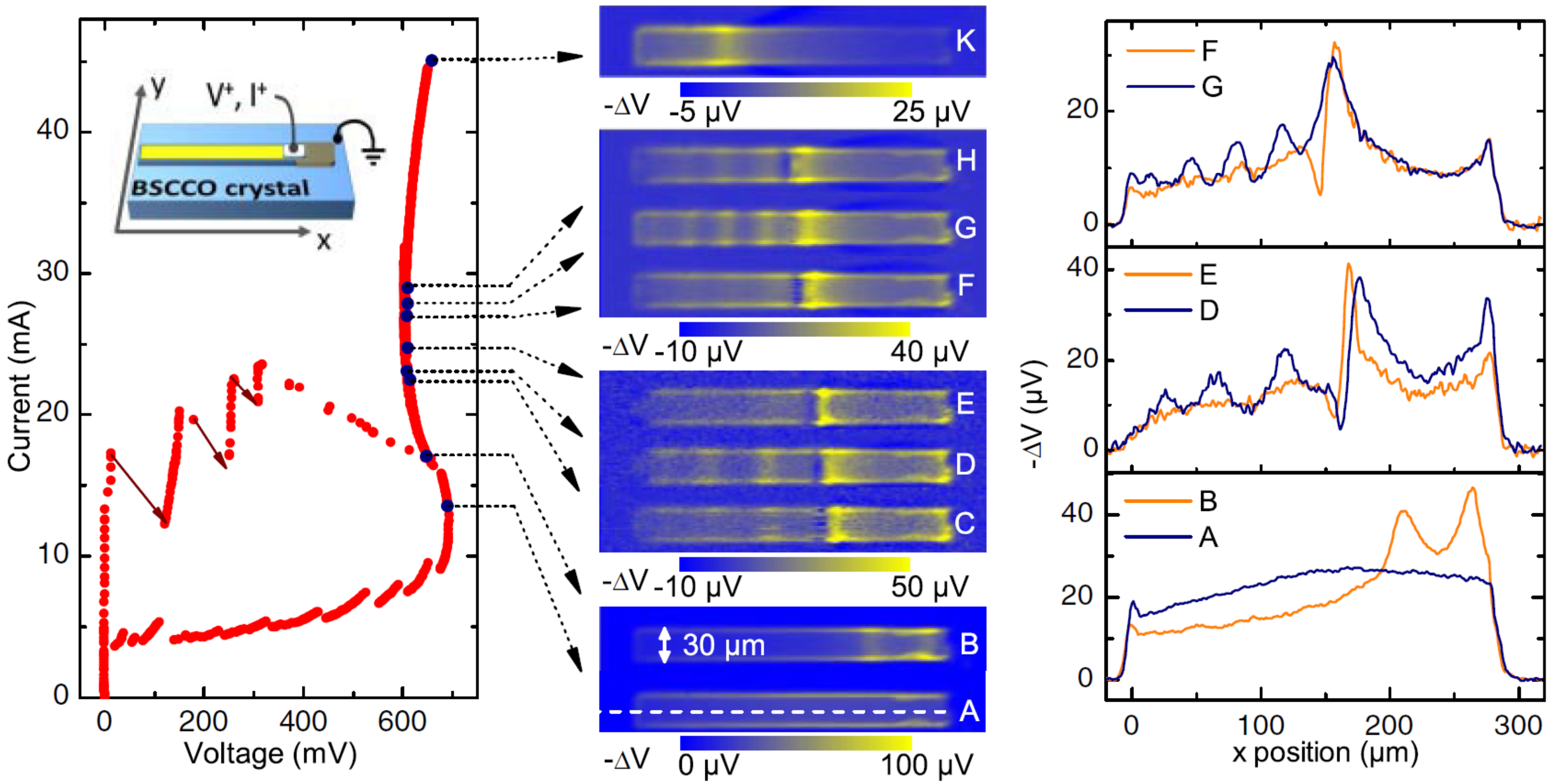

H.B.Wang et al., PRL 102, 017006 (2009)

Calculation of flux-flow emission from stacked junctions

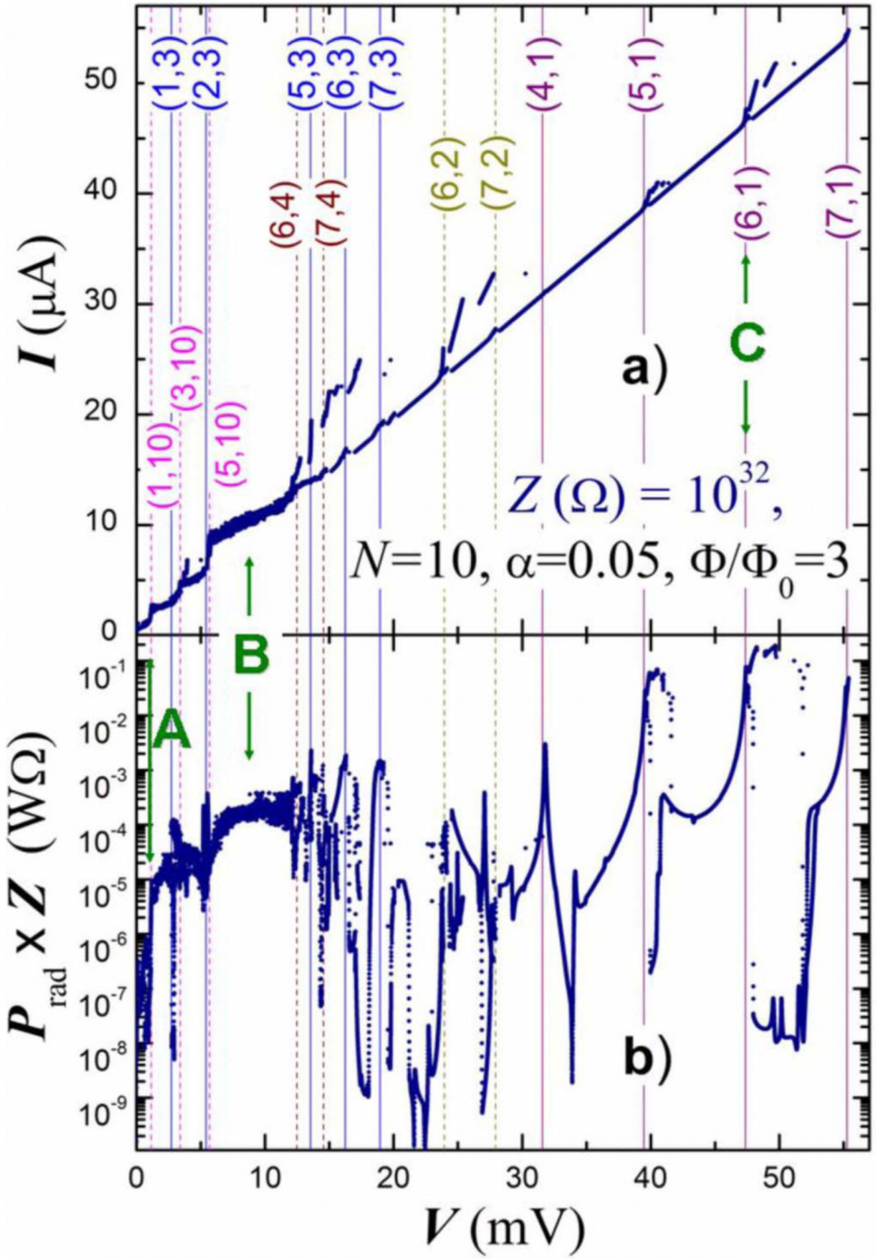

VK, PRB 82, 134524 (2010)

Zero-field emission via breather type self-oscillations

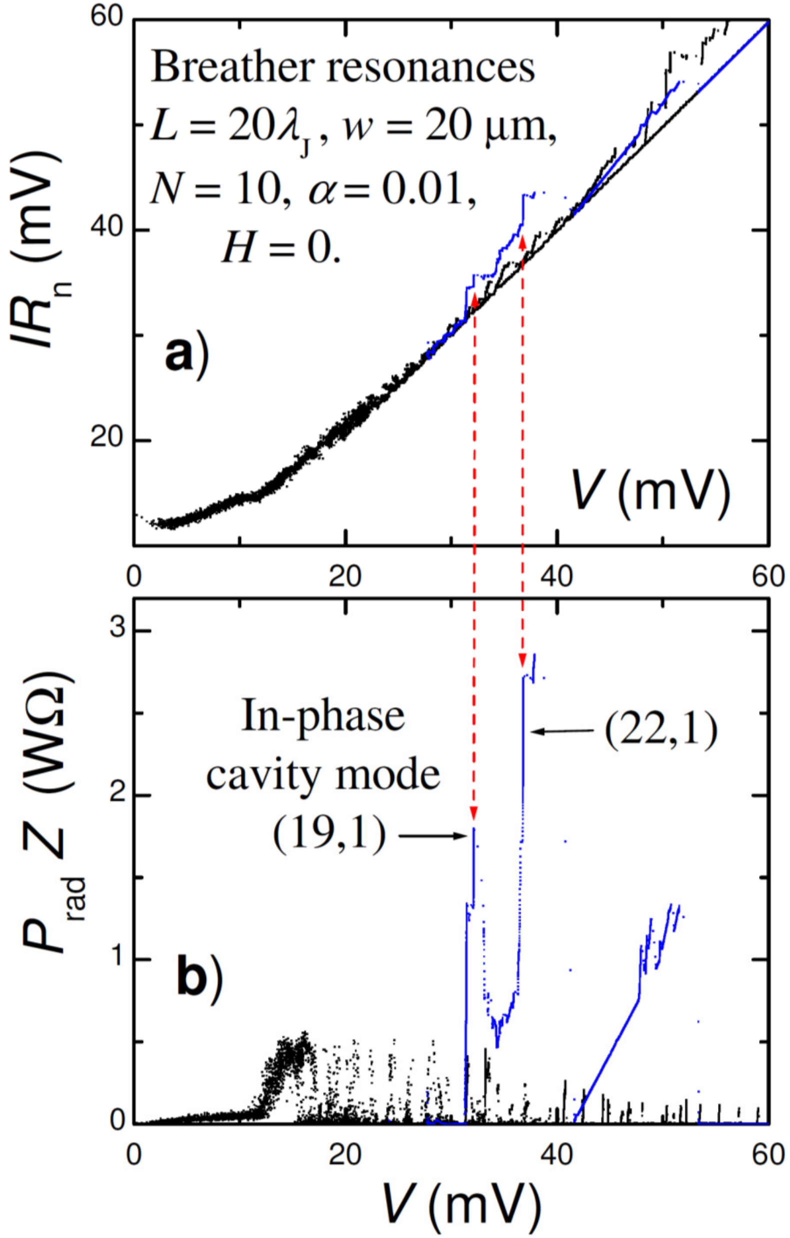

VK, PRB 83, 174517 (2011)

Motivation for the search of emission from SMALL Bi-2212 mesas

Advantages of small:

- High uniformity of junctions (no deffects)
- High Q of geometrical resonances (~1/L)
- Low heating = high frequency up to Δ ~ 30 meV > 15 THz
- Fully (?) understood theoretically: MUST emit!

II. But No emission in mesas with N ~ 20-50 (P<1pW)

III. Detection of emission from SMALL-but-HIGH mesas with N >100 with f ~ 1-11 THz

THz generation by small-but-high mesas

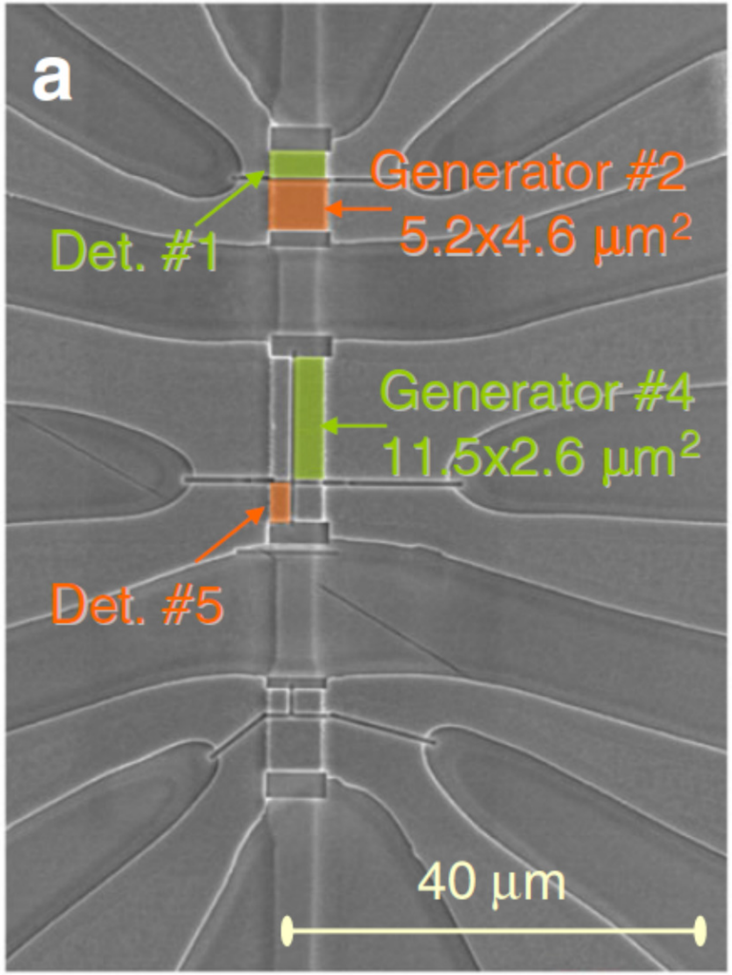

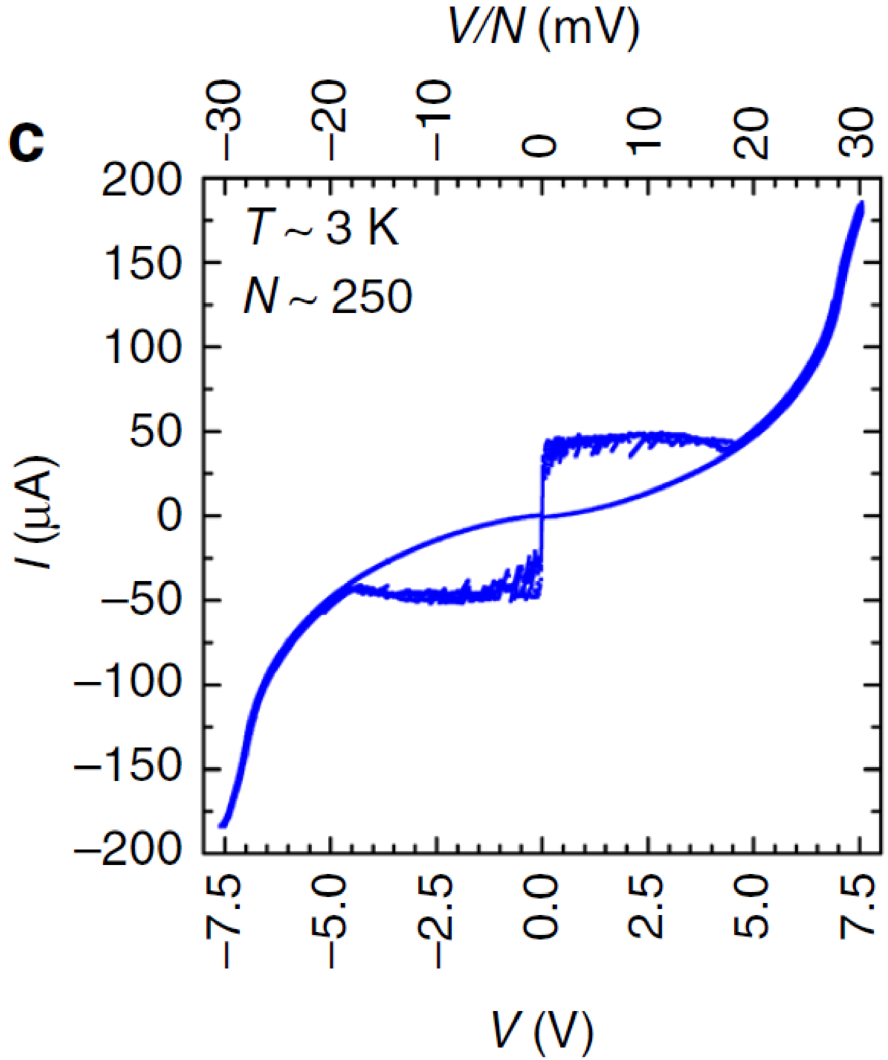

From E.A. Borodianskyi & VMK, *Nat. Commun.* **8**, 1742 (2017)

Detection of emission: Surface junction as a switching current detector

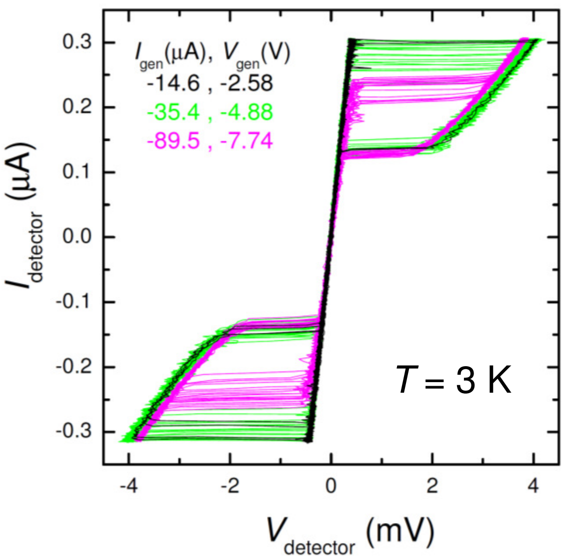

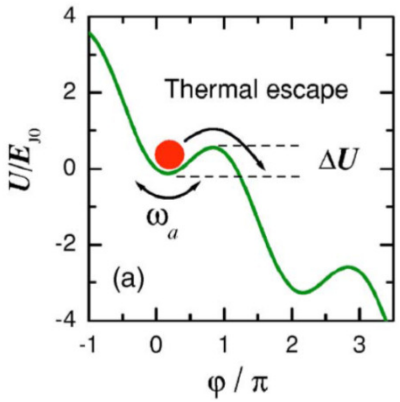

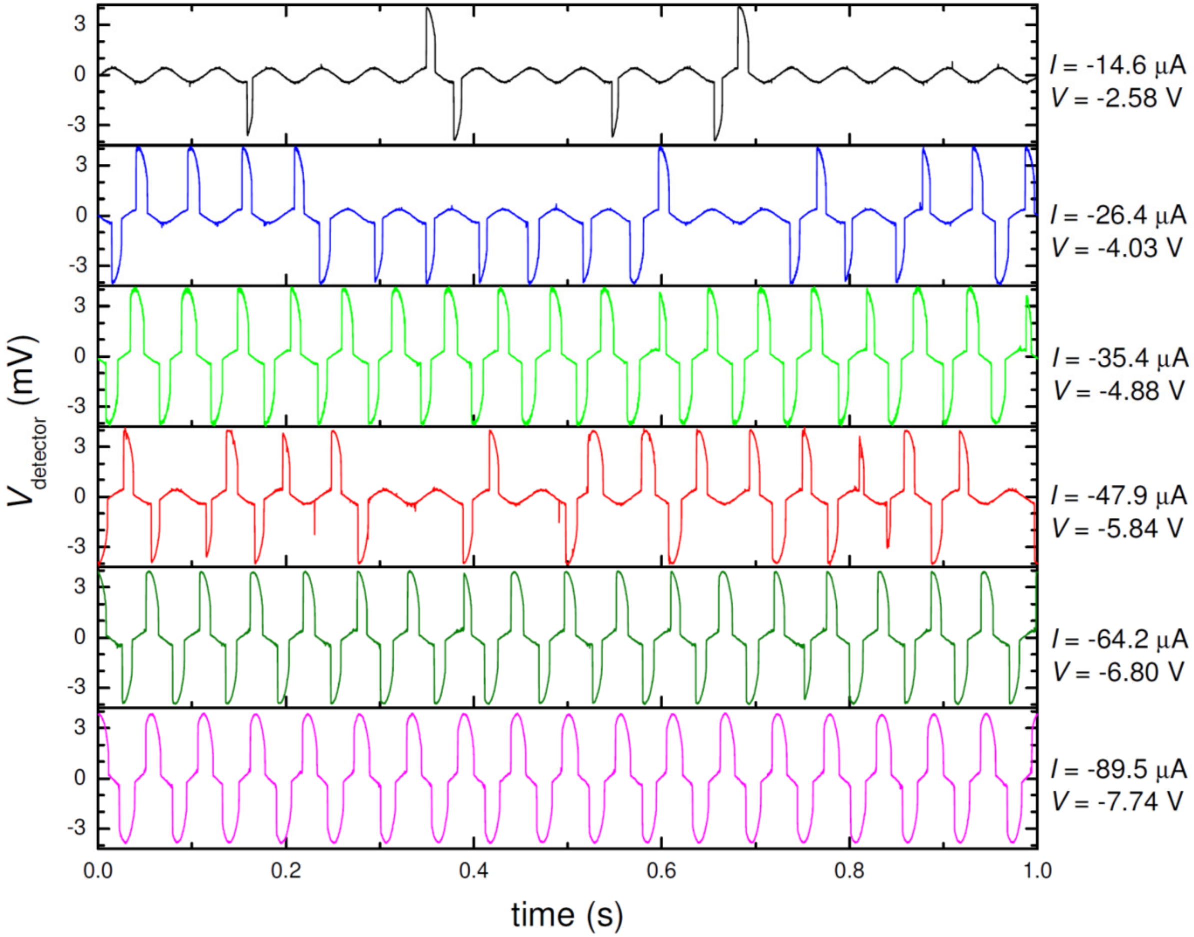

$$\Delta U \simeq \frac{4\sqrt{2}}{3}\left(1-\frac{I}{I_0}\right)^{3/2}\frac{\Phi_0 I_0}{2\pi} \qquad \Delta t = V_c/\Phi_0$$

Switching condition:

$I = I_{dc} + I_{rf} = I_{sw}(T)$

$I_{rf} = I_{sw} - I_{dc} \sim 0.1\ \mu A$

Absorbed power: $P_a \simeq \frac{2\sqrt{2}}{3\pi}\left(1-\frac{I_s}{I_0}\right)^{3/2} I_0 V_c$ ~1 nW

Emitted power ~1 mW (BWO – test experiment)

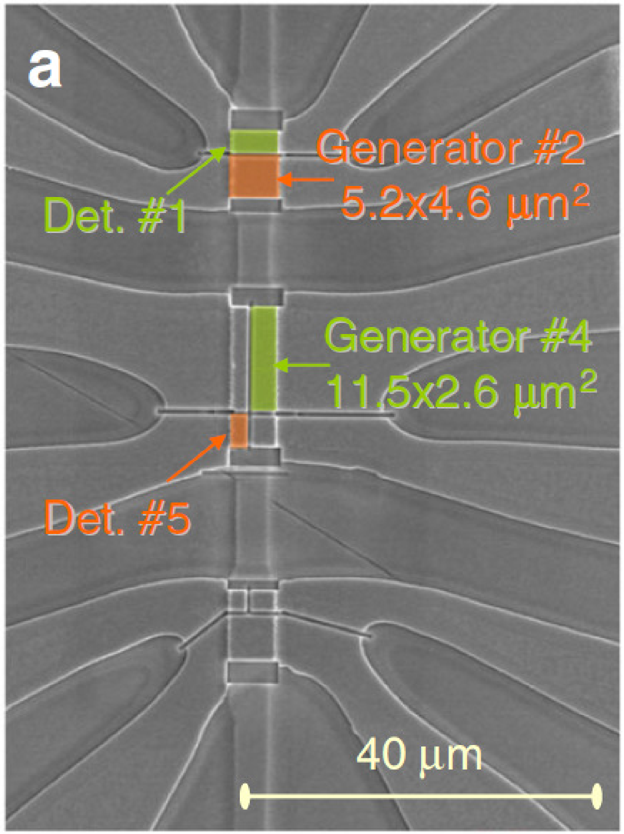

From E.A. Borodianskyi & VMK, *Nat. Commun.* **8**, 1742 (2017)

Generator 2, Detector 5

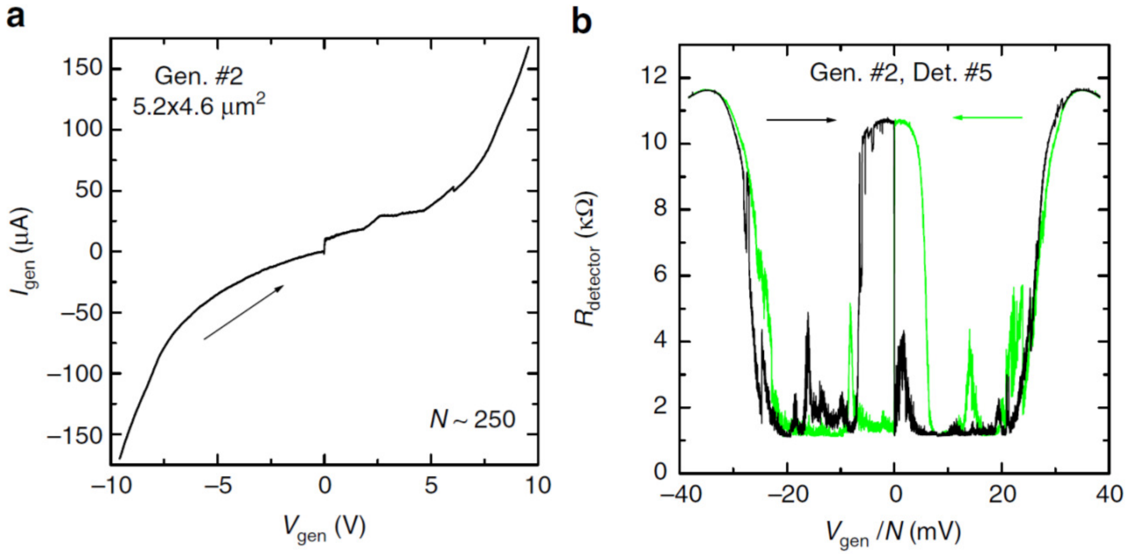

Generator 4, Detector 1

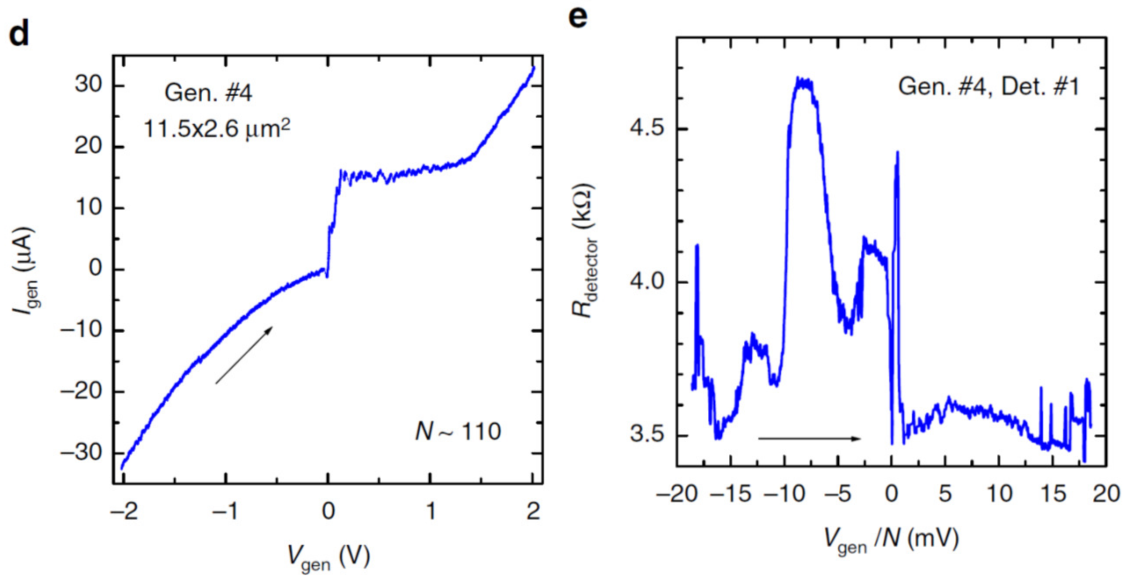

Emission occurs only when all IJJs are active - superradiant

Estimation of in-phase geometrical resonances

$$f(m,n) = \frac{c_1}{2}\sqrt{\frac{m^2}{L_x^2}+\frac{n^2}{L_y^2}}. \qquad f = \frac{2e}{h}V \quad (\simeq 0.48359\,\mathrm{THz/mV}).$$

$$f_{(1,0)} = c_1/2L \qquad c_1(N\sim 250) \approx 0.1c \approx 3\mathrm{x}10^7\ \mathrm{m/s}$$

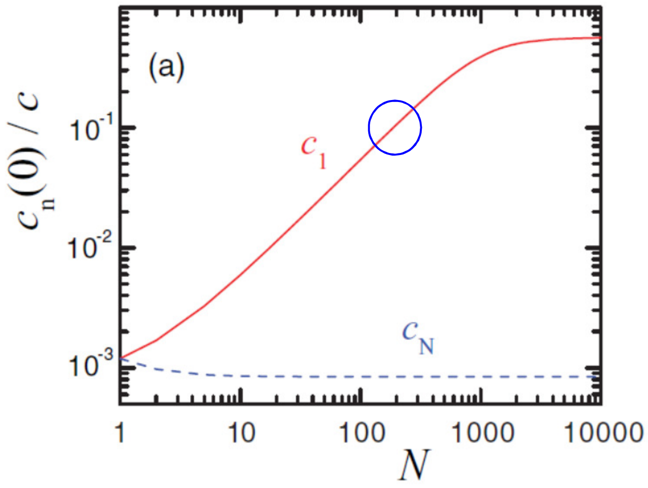

Katterwe, VMK, PRB 84, 214519 (2011)

Gen#2: L≈5μm, $f_{(1,0)}$ ≈ 3 THz

c

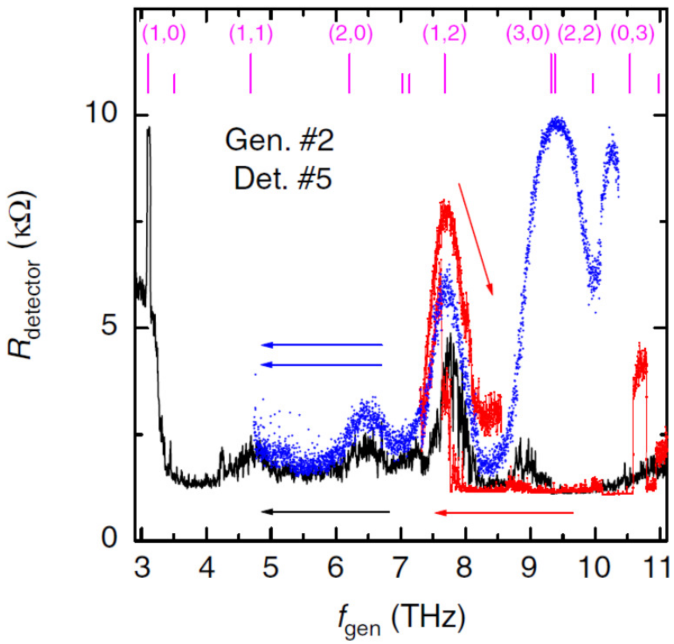

Gen#4: L≈12μm, $f_{(1,0)}$ ≈ 1.3 THz

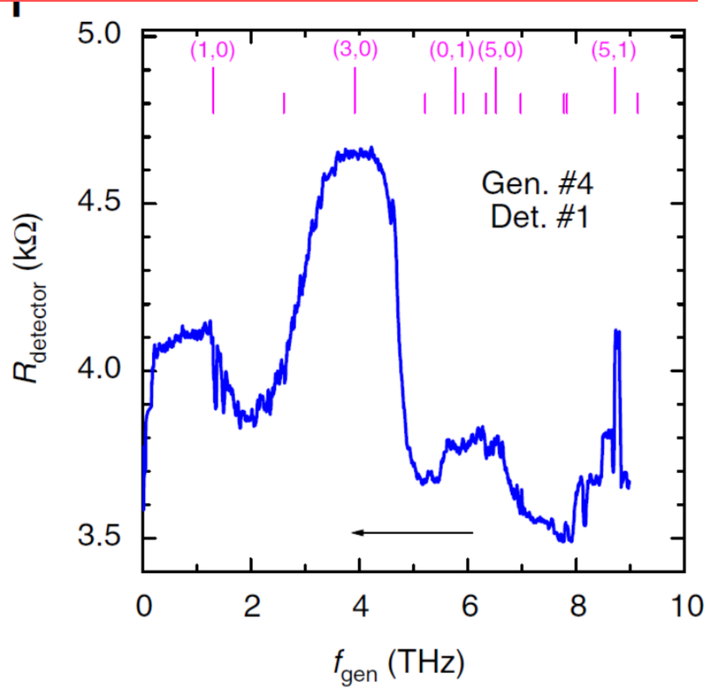

Efficiency: P_{rf} ~ 1 μW, P_{dc} ~ 0.1 mW -> 1%

Power density (5x5 μm²) : ~ 4 W/cm²

Scaled P to 200x200 μm² : ~ 1.6 mW

Conclusion- 1

AC-Josephson emission of EM waves from Bi-2212 mesas: Large mesas – high power, low-*f* due to heating. Small-but-high mesas emit high-*f* with high efficiency.

- **Emission at in-phase cavity modes = coherent emission**
- **Small = Low heating = high *V* = high *f***
- **Record high frequency and fr. span 1-11 THz,**
- **Close to theoretical limit Δ ~ 15 THz**
- **Achieved (unoptimized) power density ~ to large mesas.**
- **Tunable in the whole THz gap region and beyond by geometry and Bias**
- **Seemingly, there is a threshold *N* ~ 100**
- **Not just N^2 effect**
- **Not present in CSGE theory. Why? Power-synchronization, Cascade amplification, Collective cavity pumping - stimulated emission…**

See: E.A. Borodianskyi & VMK, *Nat. Commun.* **8**, 1742 (2017)

II. Semi-Josephson generation of phonons by the ac-Josephson effect in junctions with polar barrier (electrostriction)

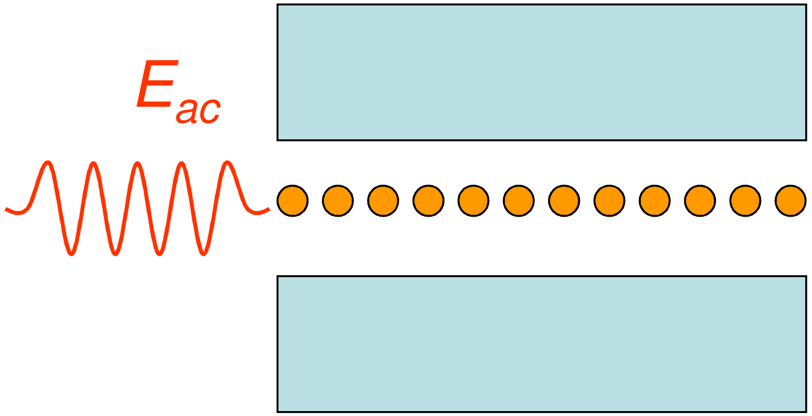

First demonstration: In Low-Tc:

H. Kinder, Phys. Rev. Lett. 28, 1564 (1972)

In High-Tc (Bi-2212 and Tl-2212):

A.Yurgens, Supercond. Sci. Technol. 13, R85 (2000);

K. Schlenga et al., Phys.Rev.B 57, 14518 (1998).

#	V (mV)	ω_{LO} (cm^{-1})	type	symmetry	assignment
1	6.0	97	IR	A_{2u}	Bi':Cu1CaSr
2	7.8	126	Raman	A_{1g}	Cu1Sr
3	10.5	169	IR	A_{2u}	Sr:Cu1'
4	11.2	181	Raman	A_{1g}	Sr:Cu1'
5	14.5	234	IR	A_{2u}	Ca:Sr'
6	20.4	329	IR	A_{2u}	O3O1
7	22.8	368	IR	A_{2u}	O1':CaO3
8	25.5	411	Raman	A_{1g}	O1:Sr'

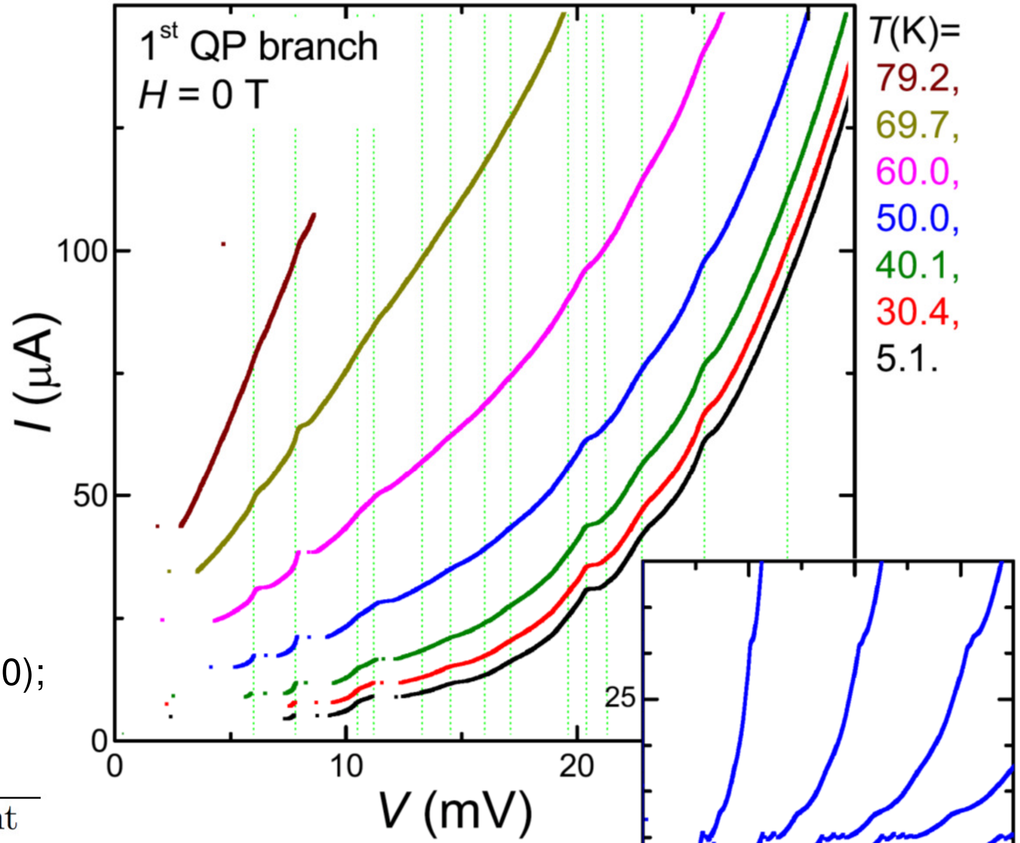

S.O.Katterwe, et al, Phys. Rev. B 83, 100510(R) (2011).

In $Bi_2Sr_2CaCu_2O_{8+x}$ single crystal – sharp, high quality phonon resonances (7 IR + 7 Raman optical phonons)

Tuning the phonon wavelength by magnetic field

H=0

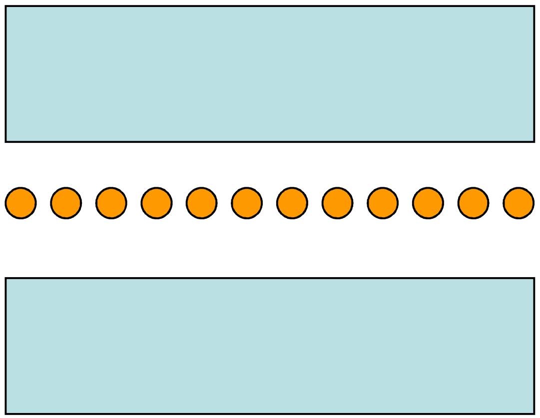

$$k = 0$$

Longitudinal Optical (LO) Phonons,

C.Preis, C.Helm, et al Physica C 362, 51 (2001)

H>0

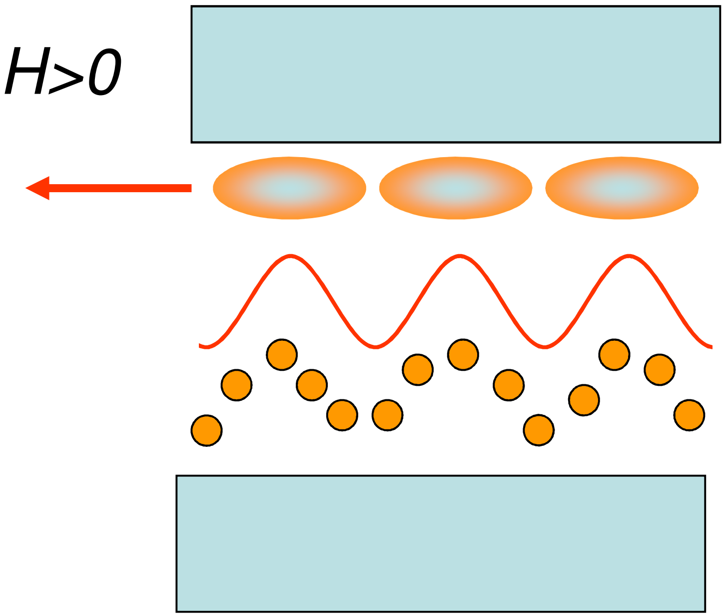

Transverse Optical (TO) Phonons

Direct determination of the dispersion relation via the velocity-matching resonance:

$$\boxed{\begin{aligned} k &= 2\pi H s/\Phi_0 . \\ \omega &= 2\pi V^*_{\mathrm{FF}}/\Phi_0 \end{aligned}}$$

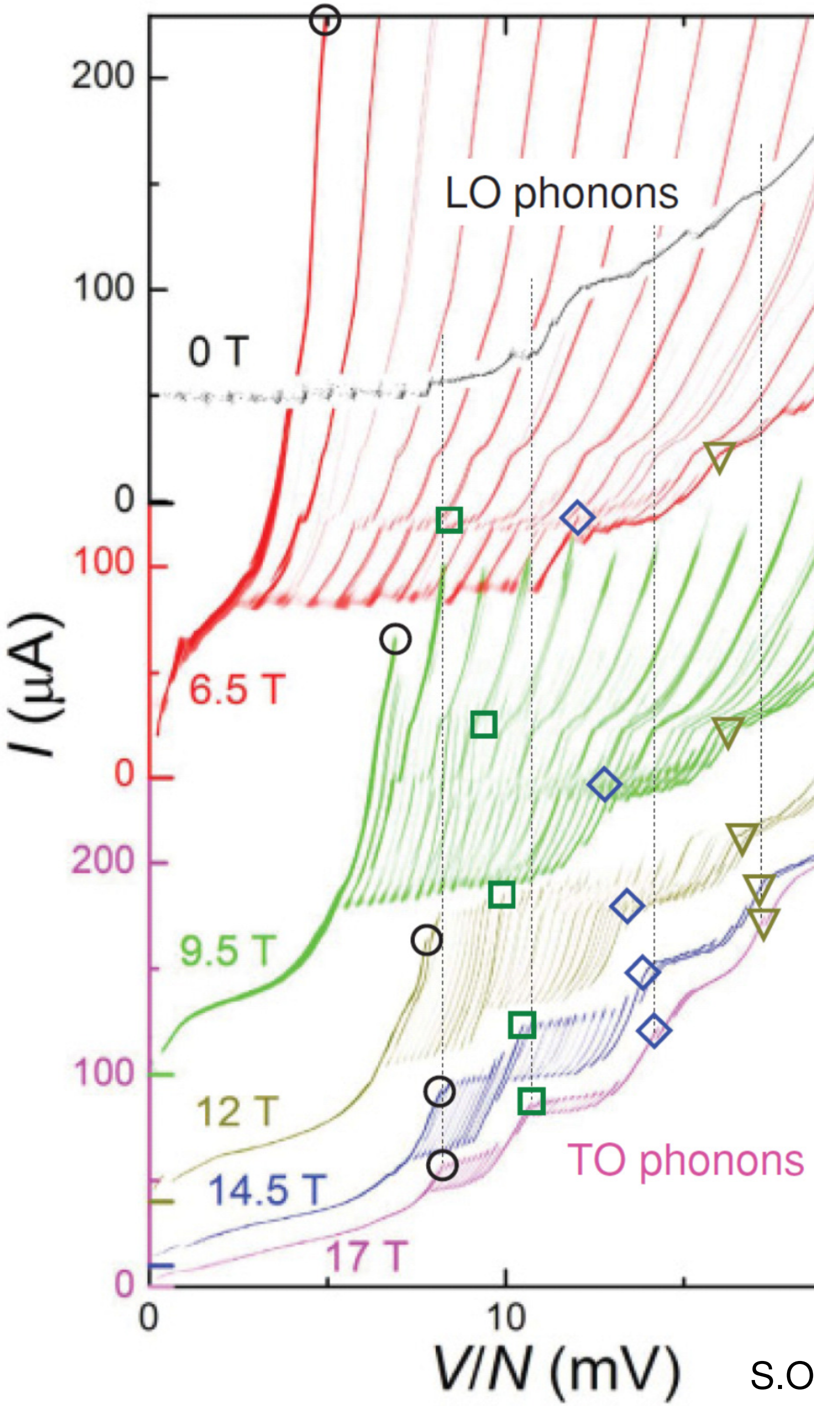

Power density at phonon - flux-flow resonances: ~1-10 kW/cm^2

S.O.Katterwe, et al, PRB 83, 100510(R) (2011)

Phonon-Polariton dispersion

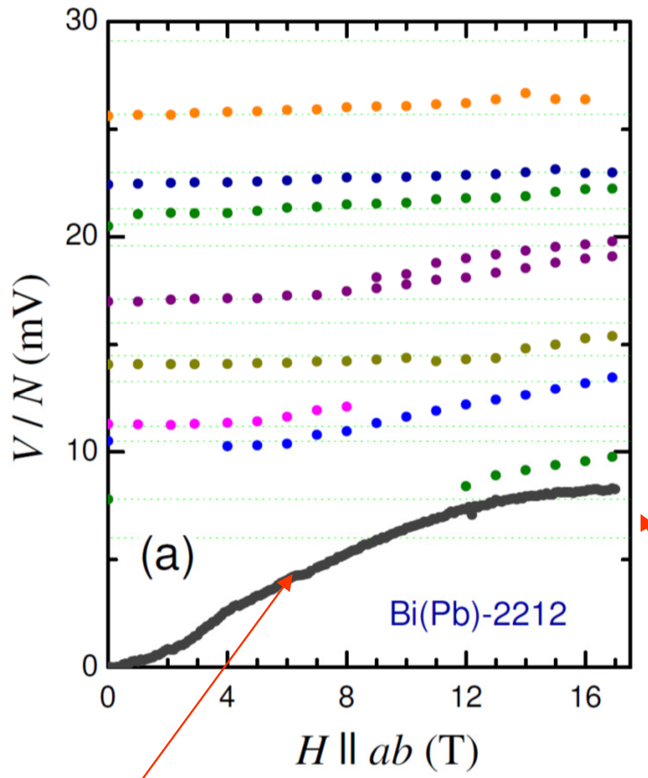

$$\omega = c_{\mathrm{n}}\, k$$

I… nation of the
c… tion via the
velocity-matching resonance:

$$\boxed{\begin{aligned} k &= 2\pi H s/\Phi_0. \\ \omega &= 2\pi V^{*}_{\mathrm{FF}}/\Phi_0 \end{aligned}}$$

$$\epsilon_{\mathrm{r}}(\omega) = \epsilon_\infty + \sum_j \frac{\omega_{\mathrm{TO}j}^2 S_j}{\omega_{\mathrm{TO}j}^2 - \omega^2 - i\gamma_j\omega}$$

$d\omega/dk \to 0$

Slow light – a fingerprint of Phonon-Polaritons

III. Non-Josephson emission upon non-equilibrium quasiparticle relaxation

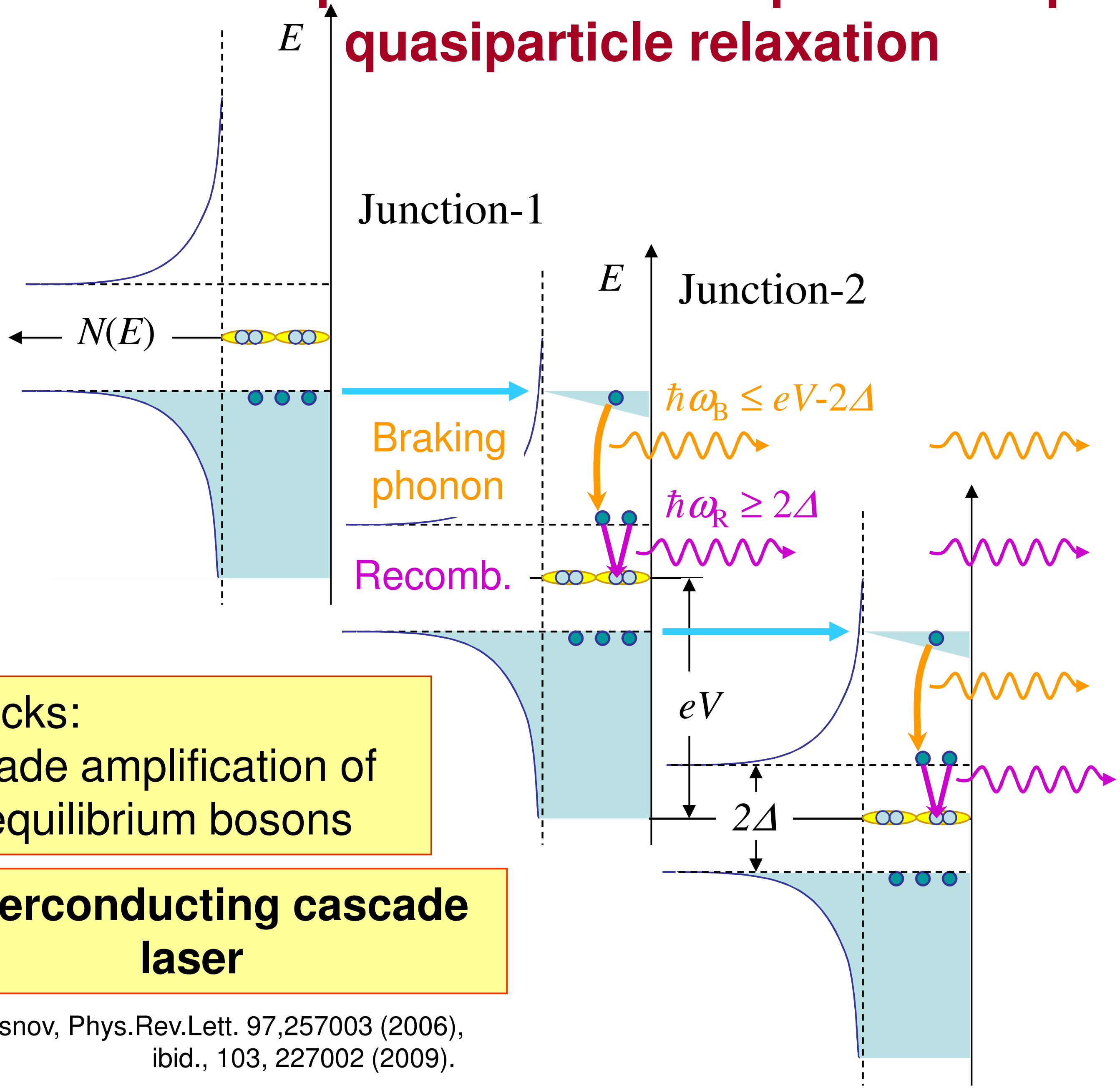

In stacks:
Cascade amplification of non-equilibrium bosons

Superconducting cascade laser

V.M.Krasnov, Phys.Rev.Lett. 97,257003 (2006), ibid., 103, 227002 (2009).

Quantum cascade laser

J.Faist, et al., Science 264 (1994) 553

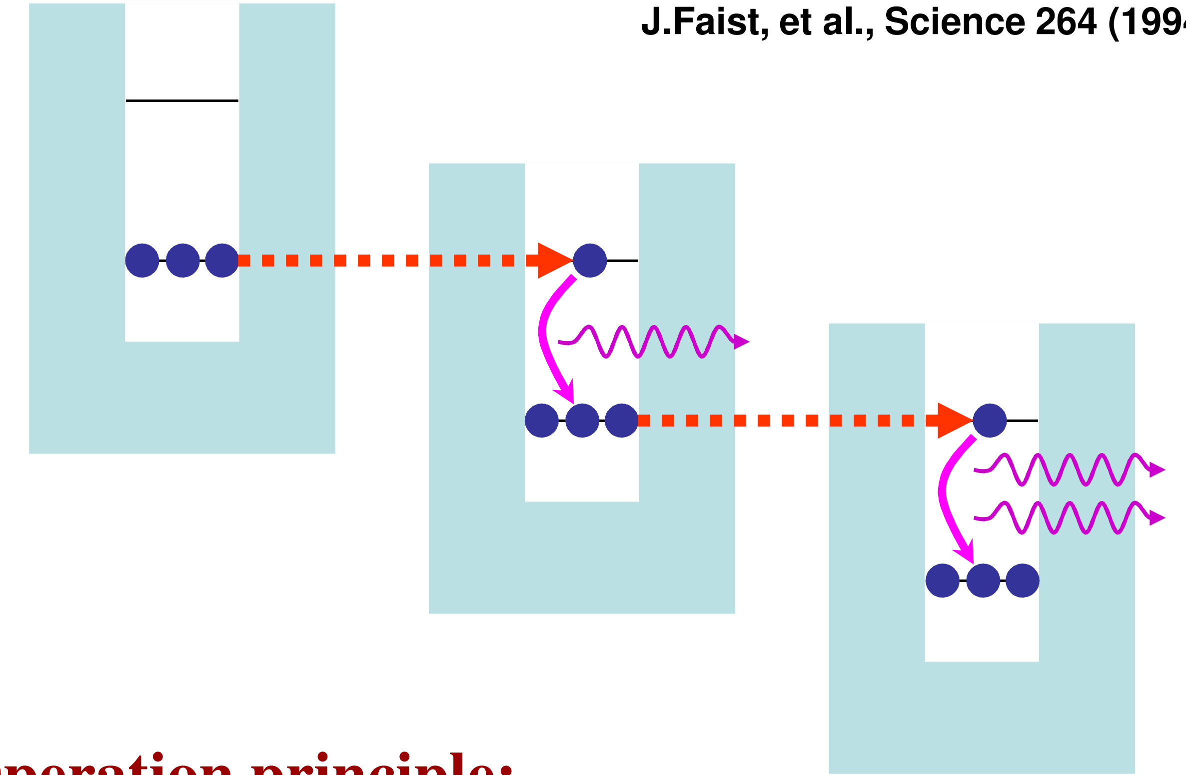

Operation principle:

- Coupled quantum wells
- Population inversion by resonant tunneling
- Cascade amplification of light intensity

Effect of stacking in semiconducting heterostructure lasers

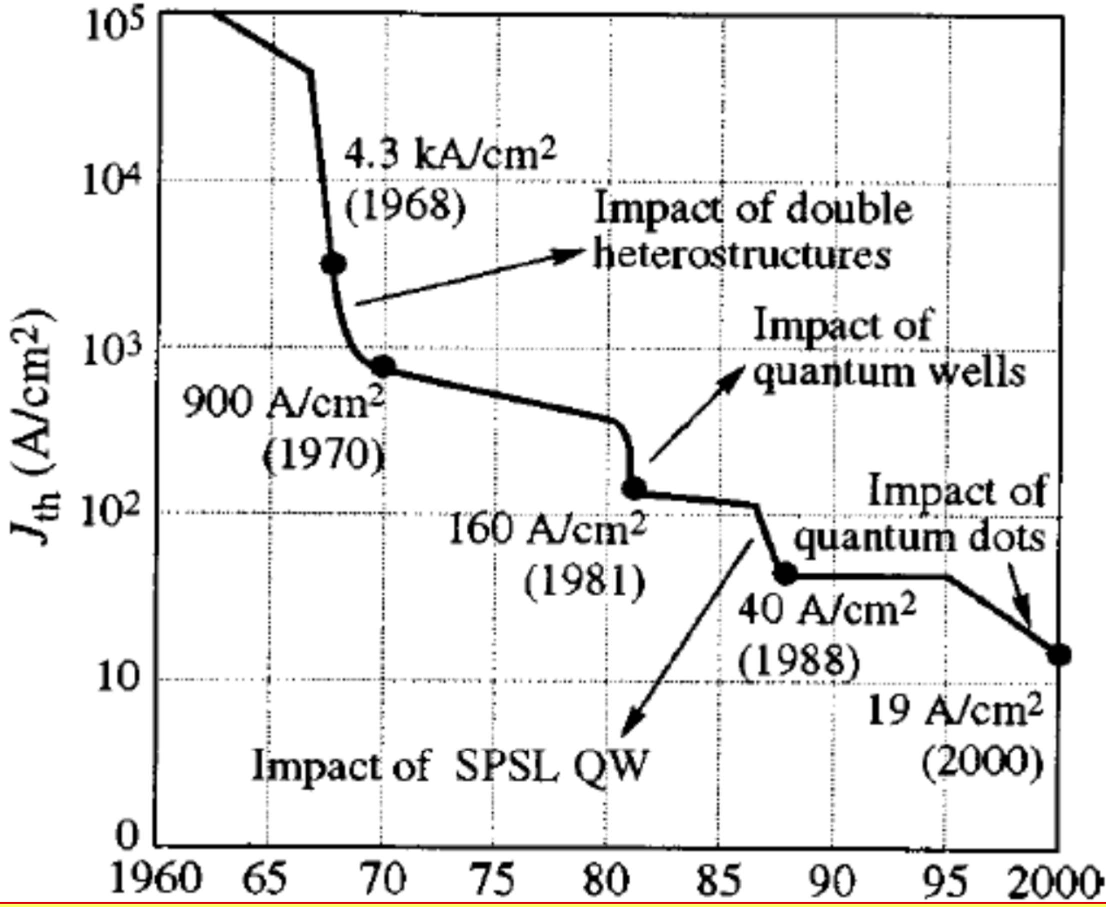

Stacking leads to :

QP confinement (no leakage)

Cascading

Superconducting gap unlike the semiconducting gap is naturally placed in the THz frequency range

Factors enhancing nonequilibrium effects in IJJs

Very rough estimation: $DoS \cdot \delta f \sim I \cdot \tau \Rightarrow \delta f \sim \dfrac{J \cdot \tau}{d \cdot dos(cm^3)}$

	$Al/AlO_x/Al$	$Nb/AlO_x/Nb$	IJJs Bi-2212
J_c (A/cm^2)	~10	10^2-10^3	$3x10^2$-$3x10^3$
Δ (meV)	0.4	1.4	30-40
$J(V_g)$ (A/cm^2)	~10	10^2-10^3	~ 10^3-10^4
dos($1/eVcm^3$)	~$2x10^{22}$	~$2x10^{22}$	~10^{22}
d (nm)	~100	~200	~0.4
τ (ns)	~1000	~0.2	~$2x10^{-3}$ (opt.)
δf (V_g) (a.u.)	~50	0.05-0.5	5-50

Additional effects of stacking

Bosons	Cascading	N = 10-10^3
QPs	Confinement	no leakage

Kinetic balance equations

$$\frac{\partial \delta N(E,\Omega)}{\partial t} = \frac{\partial \delta N}{\partial t}_{(rel)} + \frac{\partial \delta N}{\partial t}_{(inj)} + \frac{\partial \delta N}{\partial t}_{(esc)}$$

Tunnel QP injection rate **(bias dependent)**

$$\frac{\partial \delta N(E)}{\partial t}_{(inj)} = \frac{\Delta}{e^2 R_n} \frac{dE}{\Delta} \rho(E)\rho(E-eV)\left[f(E-eV)-f(E)\right]$$

QP escape rate (via tunneling)

$$\frac{\partial \delta N(E)}{\partial t}_{(esc)} = -\frac{\Delta}{e^2 R_n} \frac{dE}{\Delta} \rho(E)\rho(E+eV)\left[f(E)-f(E+eV)\right]$$

Phonon injection rate
(bias independent)

$$\frac{\partial \delta N(\Omega)}{\partial t}_{(inj)} = -\beta N_J \frac{\partial \delta N(\Omega)}{\partial t}_{(esc)}$$

Phonon escape rate

$$\frac{\partial \delta N(\Omega)}{\partial t}_{(esc)} = -\delta N(\Omega)\frac{v_s}{d}$$

Quasiparticle relaxation rate

$$\left.\frac{\partial \delta N(E)}{\partial t}\right|_{(rel)} = -\frac{4\pi V\, D_{QP}(0)dE}{\hbar}\times$$

$$\int_0^\infty d\Omega\,\alpha^2 D_{Ph}(\Omega)\rho(E)\rho(E+\Omega)\left(1-\frac{\Delta^2}{E(E+\Omega)}\right)\{f(E)[1-f(E+\Omega)]g(\Omega)-f(E+\Omega)[1-f(E)][1+g(\Omega)]\}$$

Relaxation:
absorption-emission
emission-absorption

$$+\int_0^{E-\Delta} d\Omega\,\alpha^2 D_{Ph}(\Omega)\rho(E)\rho(E-\Omega)\left(1-\frac{\Delta^2}{E(E-\Omega)}\right)\{f(E)[1-f(E-\Omega)][1+g(\Omega)]-f(E-\Omega)[1-f(E)]g(\Omega)\}$$

Recombination – pair breaking

$$+\int_{E+\Delta}^\infty d\Omega\,\alpha^2 D_{Ph}(\Omega)\rho(E)\rho(\Omega-E)\left(1+\frac{\Delta^2}{E(\Omega-E)}\right)\{f(E)f(\Omega-E)[1+g(\Omega)]-[1-f(E)][1-f(\Omega-E)]g(\Omega)\}$$

Absorption | **Spontaneous emission** | **Stimulated emission**

Phonon relaxation rate

$$\left.\frac{\partial \delta N(\Omega)}{\partial t}\right|_{(rel)} = -\frac{8\pi V\, D_{QP}(0)\,\alpha^2\, D_{Ph}(\Omega)\,d\Omega}{\hbar}\times$$

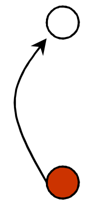

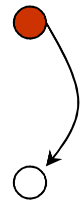

$$\int_{\Delta}^{\infty} dE\,\rho(E)\rho(E+\Omega)\left(1-\frac{\Delta^2}{E(E+\Omega)}\right)\left\{f(E)[1-f(E+\Omega)]g(\Omega) - f(E+\Omega)[1-f(E)][1+g(\Omega)]\right\}$$

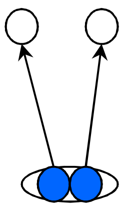

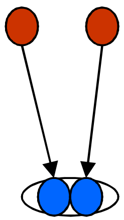

$$+\frac{1}{2}\int_{\Delta}^{\infty} dE\,\rho(E)\rho(\Omega-E)\left(1+\frac{\Delta^2}{E(\Omega-E)}\right)\left\{[1-f(E)][1-f(\Omega-E)]g(\Omega) - f(E)f(\Omega-E)[1+g(\Omega)]\right\}$$

Absorption | **Spontaneous emission** | **Stimulated emission**

Self-consistency equation:

Equilibrium $\Delta_0(T)$:

$$\frac{1}{\lambda}=\int_{\Delta_0}^{\Omega_D}\frac{\tanh(E/2kT)}{\sqrt{E^2-\Delta_0{}^2}}dE$$

$$\frac{1}{\lambda}=\int_{\Delta}^{\Omega_D}\frac{1-2f(E)}{\sqrt{E^2-\Delta^2}}dE=\int_{\Delta}^{\Omega_D}\frac{\tanh(E/2kT)}{\sqrt{E^2-\Delta^2}}dE-2\int_{\Delta}^{\Omega_D}\frac{\delta f(E)}{\sqrt{E^2-\Delta^2}}dE$$

Numerical solution for non-equilibrium Δ/Δ_0:

$$\boxed{\int_1^{\infty}\frac{\tanh\left(\frac{\varepsilon}{2}\frac{\Delta_0}{kT_c}\frac{T_c}{T}\right)-\tanh\left(\frac{\varepsilon}{2}\frac{\Delta}{\Delta_0}\frac{\Delta_0}{kT_c}\frac{T_c}{T}\right)}{\sqrt{\varepsilon^2-1}}d\varepsilon=-2\int_{\Delta}^{\infty}\frac{\delta f(E)}{\sqrt{E^2-\Delta^2}}dE}$$

QP's at the bottom of the gap are most important

Nonlinear effects at even-gap bias: Secondary nonequilibrium QP and bosons

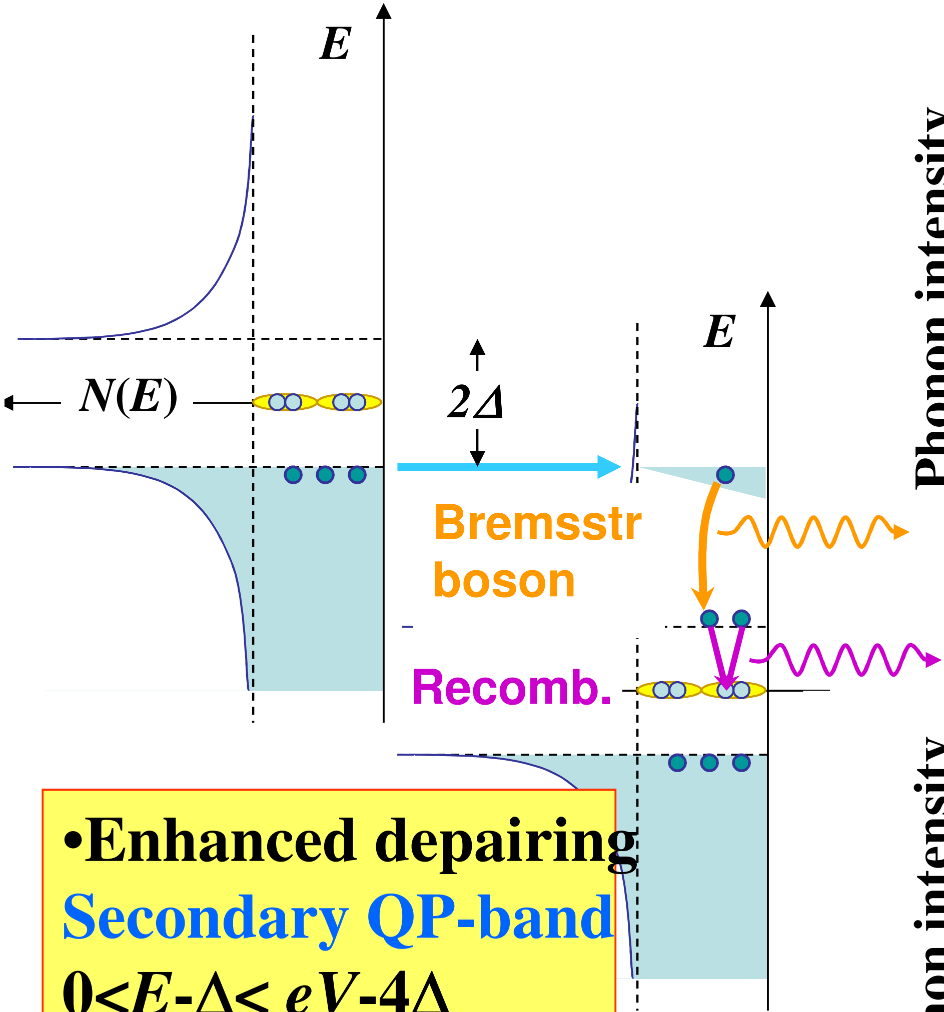

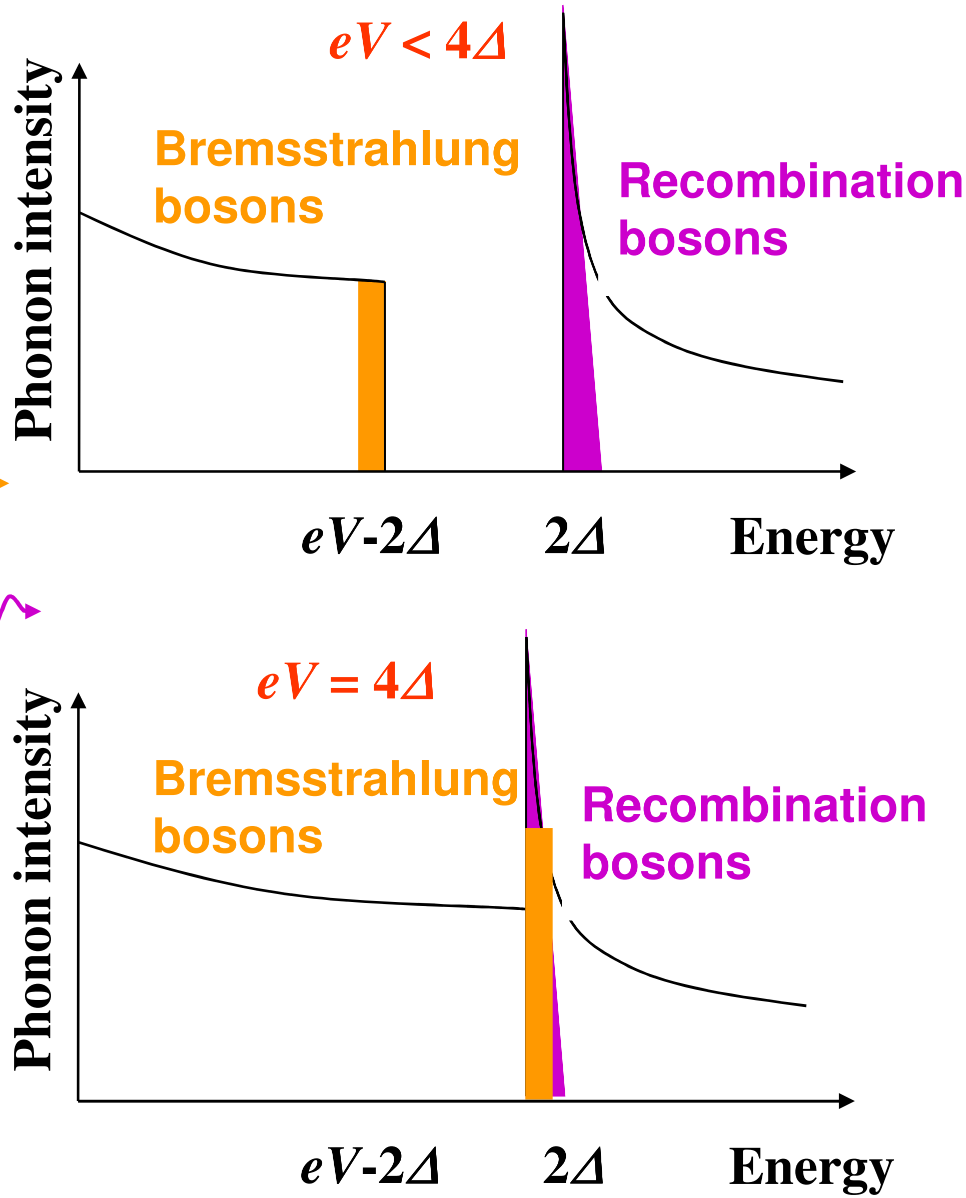

- **Enhanced depairing**
  Secondary QP-band
  $0<E-\Delta< eV-4\Delta$

New bands appear at $eV=2n\Delta$

Stimulated emission

Observation of even-gap peculiarities in Bi-2212 intrinsic tunneling characteristics

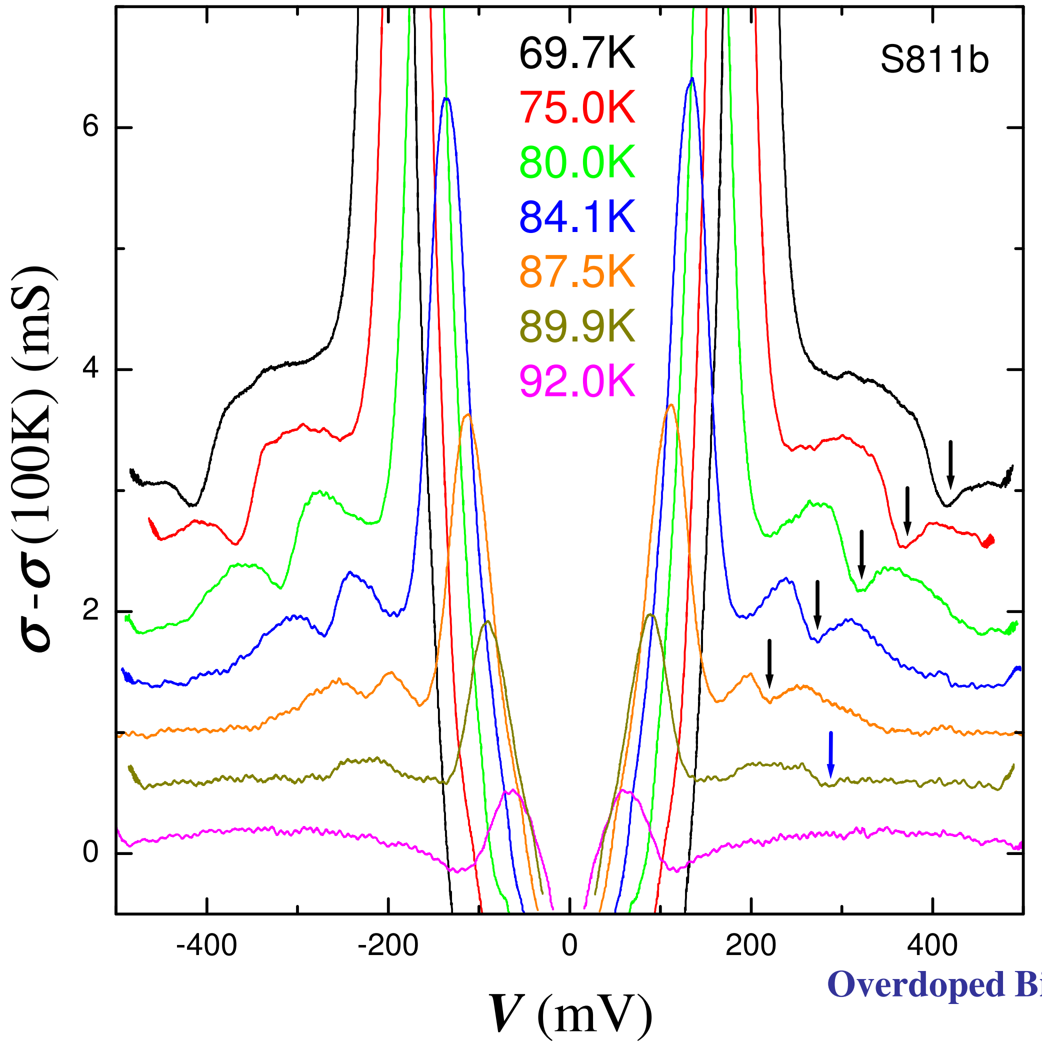

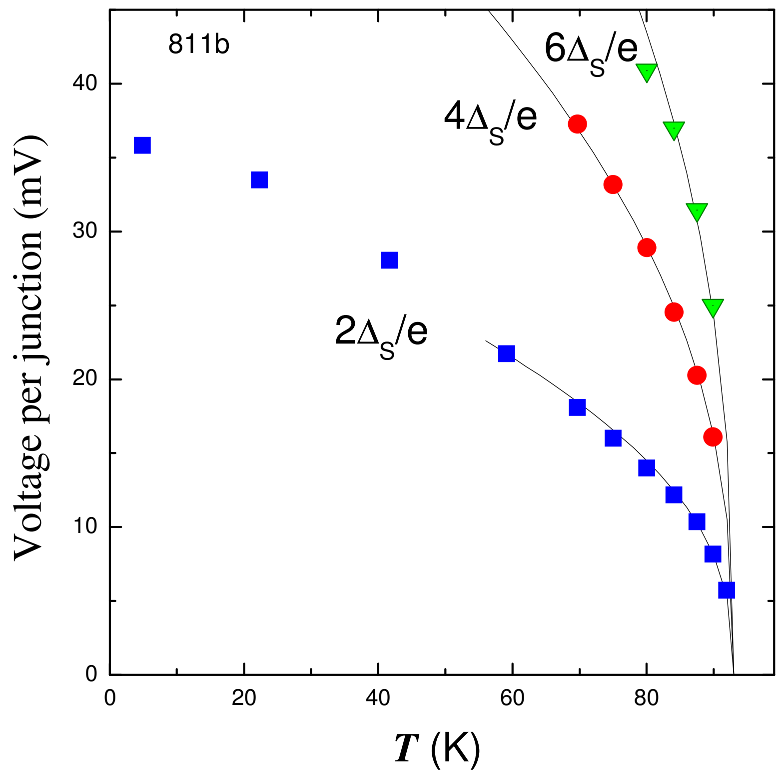

Overdoped Bi-2212

V.M.Krasnov, Phys.Rev.Lett. 97,257003 (2006)

Changing the QP injection rate:

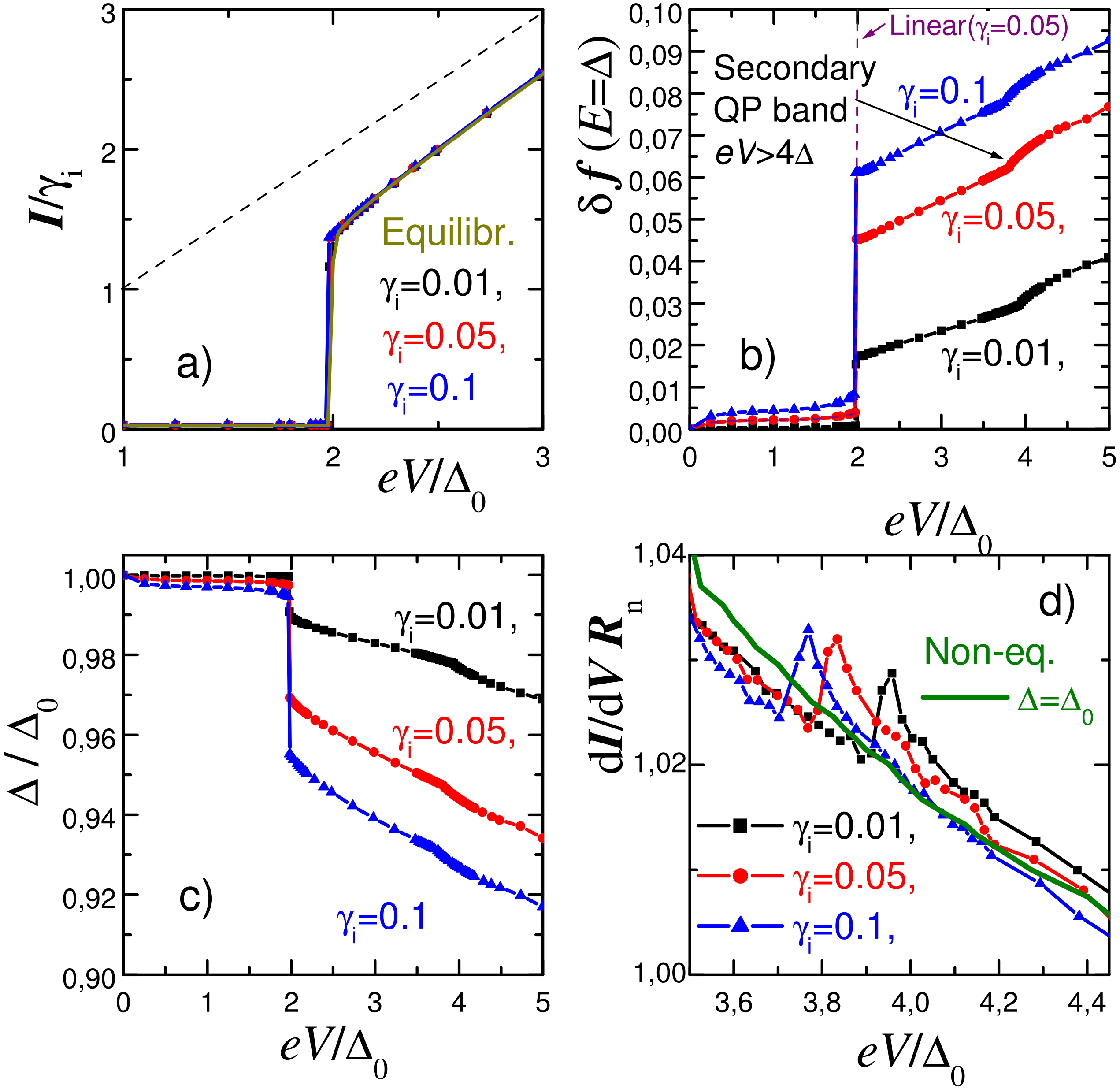

Non-linear

V.M.Krasnov, Phys.Rev.Lett. 103, 227002 (2009)

Nonequilibrium *I-V* characteristics

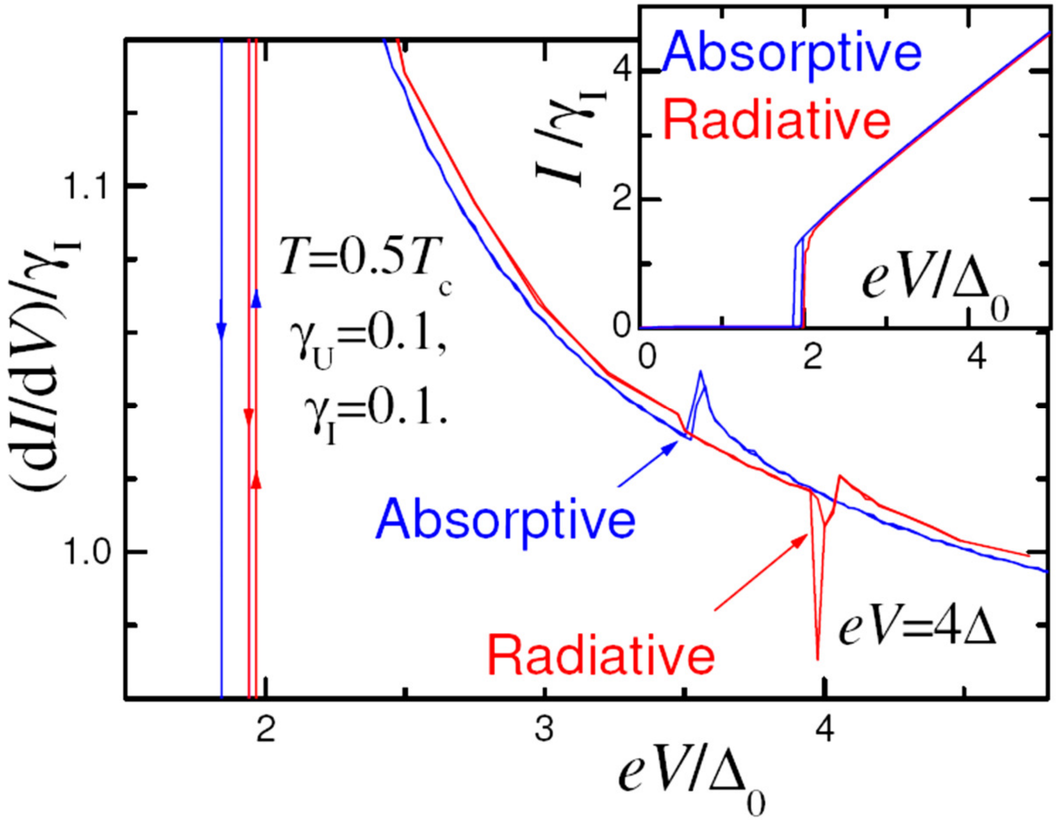

V.M.Krasnov, Phys.Rev.Lett. 103, 227002 (2009)

Note, that I-V curves are very similar for both solutions.
Therefore, power dissipation P=IV is also the same.
However, suppression of Δ is much smaller in the radiative state.
This is due to radiative cooling = ballistic boson emission from the stack.

Radiative cooling is the only heat transport mechanism considered here, κ=0.
The stack effectively (100% efficiency) converts electric power into boson emission without ac-Josephson effect.

Non-equilibrium spectroscopy as a new tool for hunting down pairing bosons

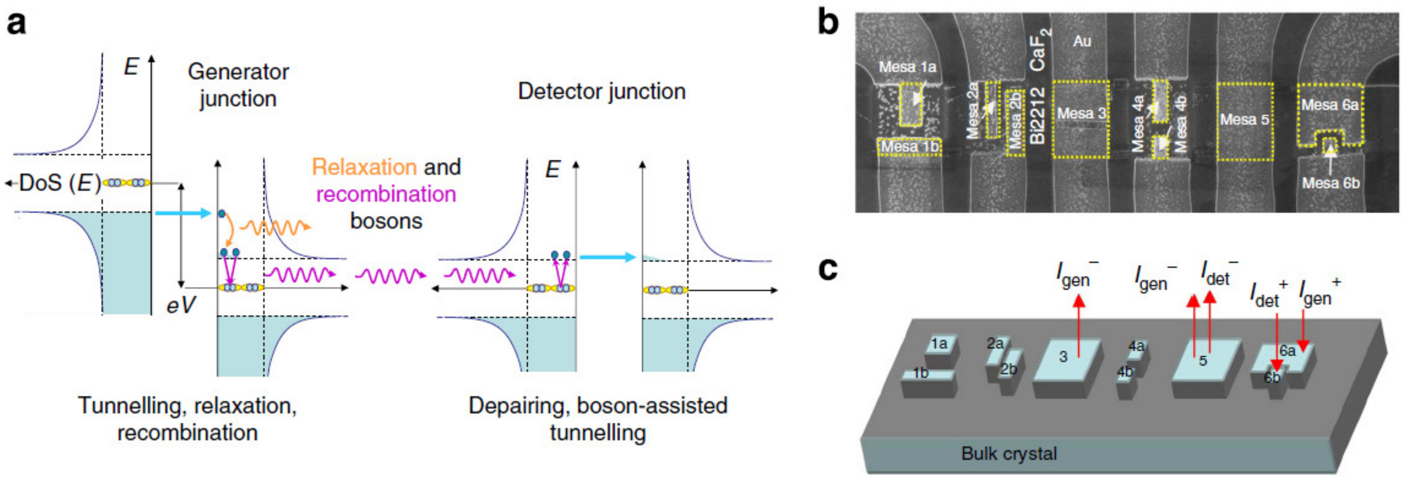

Krasnov etal.,
Nat Commun.
4, 2970 (2013)

Figure 1 | Outline of the experiment. (**a**) Tunnelling diagrams of the generator junction at the sum-gap voltage $2\Delta < eV < 4\Delta$ and the detector junction at zero bias (*s*-wave case). (**b**) Scanning electron microscope image of the studied sample. The field of view is $\sim 60 \times 22\,\mu m^2$. Ten mesa structures are marked by yellow dotted lines. (**c**) A three-dimensional sketch of the sample. Arrows indicate a bias configuration with mesa 6a as generator and 6b as detector.

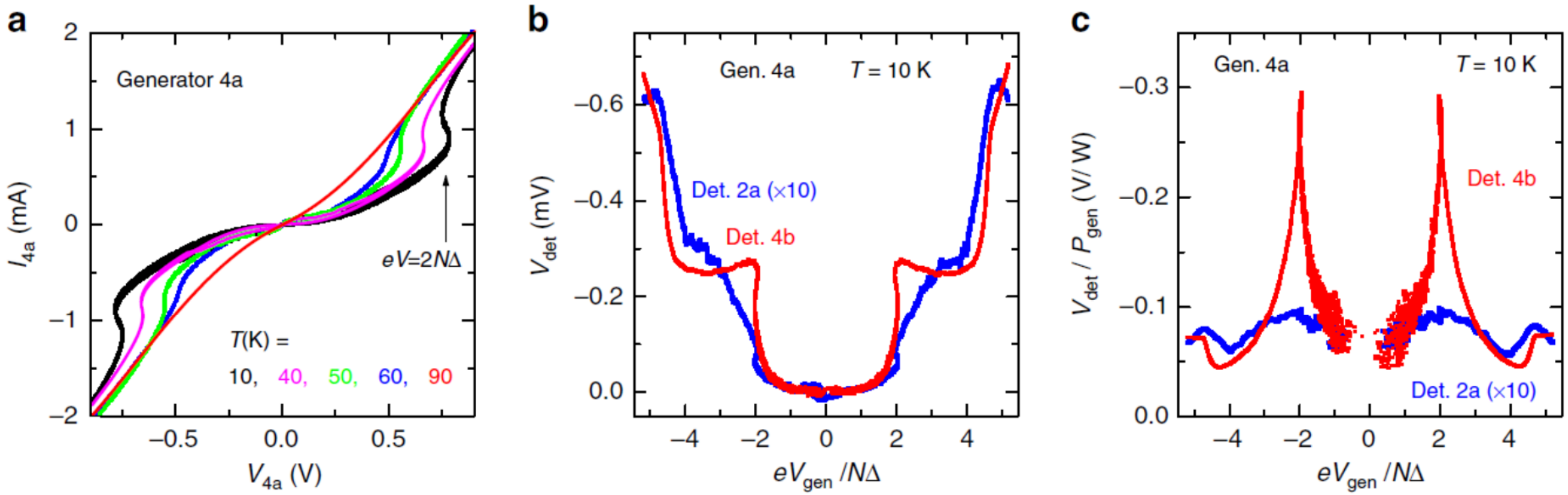

Figure 2 | Generation-detection with unbiased detector junction and simulated response. (**a**) Current-voltage characteristics of mesa 4a with $N = 12$ junctions. A sum-gap kink is clearly seen at $T < T_c \simeq 81$ K. (**b**) Voltages of the detector mesas 4b and 2a as a function of voltage in the generator 4a. It is seen that V_{det} is independent of the generator bias direction. (**c**) The detector response normalized by the total power in the generator. Characteristic spectroscopic signatures at $eV_{gen}/N \simeq 2\Delta$ and 4Δ are seen. (**d–f**) Simulation of boson generation-detection experiment (s-wave case). (**d**) Non-equilibrium boson spectra at different voltages in the generator. Relaxation $0 < \Omega < eV_{gen}/N - 2\Delta$ and recombination $\Omega > 2\Delta$ bands are seen. The bands overlap at $eV_{gen}/N = 4\Delta$. (**e**) The number of $\Omega = 2\Delta$ bosons as a function of V_{gen}. Inset shows the I–V of the generator mesa with $N = 2$ junctions. (**f**) Normalized detector response $V_{det}/P_{gen} \propto dR_{det}/dP_{gen}$ as a function of generator voltage. A primary peak in response at $eV_{gen}/N = 2\Delta$ and a secondary dip/upturn at $eV_{gen}/N \simeq 4\Delta$ indicate onset of pairbreaking by recombination and relaxation bosons, respectively.

Krasnov etal., Nat Commun. 4, 2970 (2013)

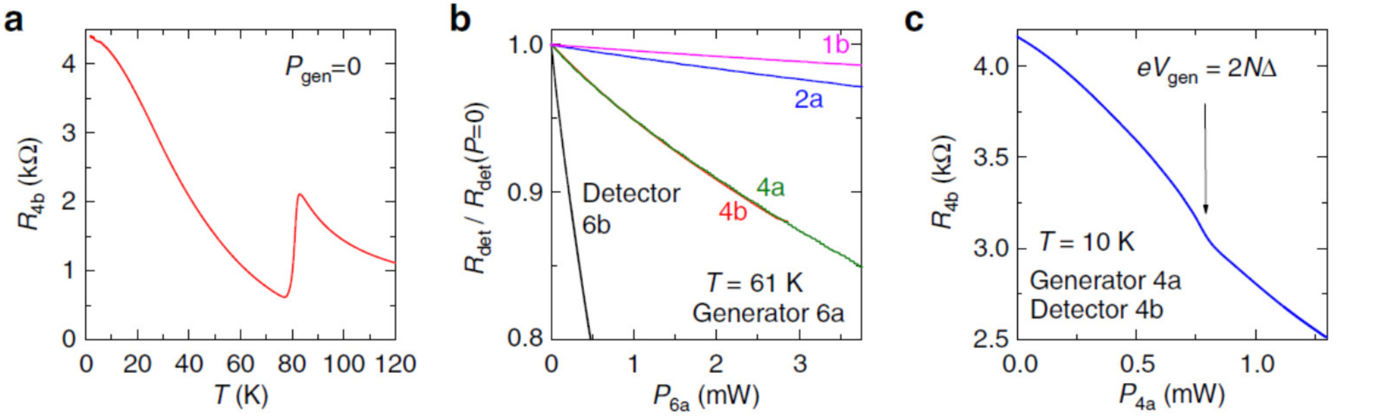

Figure 3 | Generation–detection experiment with ac-biased detector junction. (**a**) Temperature dependence of the equilibrium ac resistance of the mesa 4b. (**b**) Normalized resistances of different detector mesas at $T = 61$ K as a function of power in the generator mesa 6a. (**c**) Resistance of the detector mesa 4b at $T = 10$ K as a function of power in the generator mesa 4a. (**d**) $dI/dV(V)$ characteristics of the generator mesa 4a at different T. Peaks at sum-gap voltages are clearly seen. (**e**,**f**) Normalized detector responses of mesas 4b and 2a as a function of voltage in the generator 4a at different T. Peak responses occur at the sum-gap voltages in the generator.

Krasnov etal., Nat Commun. 4, 2970 (2013)

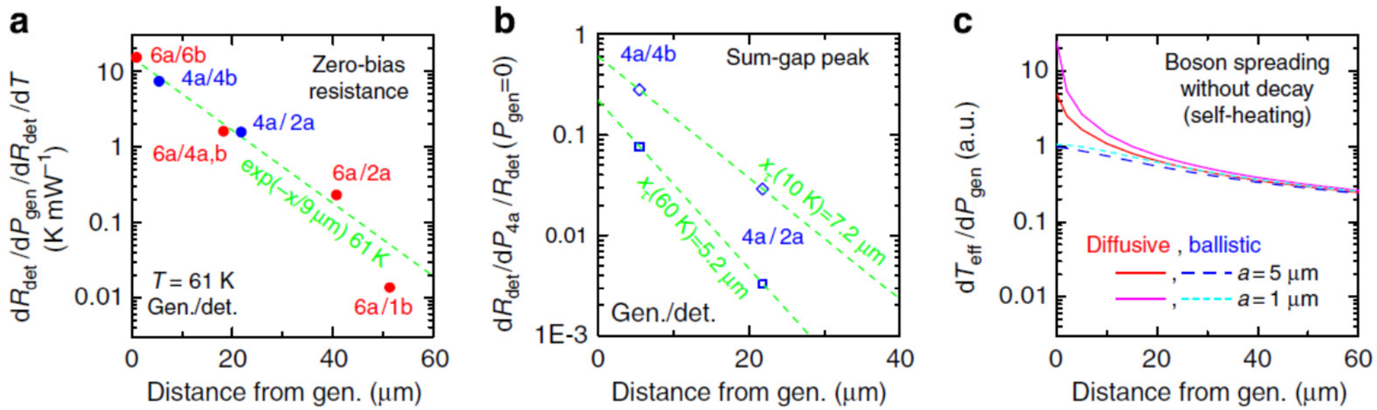

Figure 4 | Spatial dependence of detector response. (**a**) Measured spatial dependence of normalized detector responses at zero-bias $V_{gen} \to 0$ and $T = 61$ K. (**b**) Spatial dependencies of peak amplitudes in detector responses at sum-gap voltages in the generator. Note the exponential decay of detector responses with the characteristic decay length $x_\tau \sim$ µm. (**c**) Simulated temperature distribution on heat (phonon) spreading without decay (infinite bosonic lifetime). Note a significantly weaker spatial dependence than in the experiment.

Conclusions

Intrinsic Josephson junctions in cuprates are interesting as possible candidates for coherent THz sources.

- **Unlimited amount of high quality stacked Josephson junctions ~700/μm**
- **Several mechanisms of emission:**
- **Coherent superradiant ac-Josephson emission (FFO)**
- **Zero-field emission via breather type self-oscillations**
- **TUNABLE CW operation up to Δ ~ 30 meV > 15 THz**

- **Ionic single crystals – high quality phonons + polarization = Monochromatic phonon polariton emission via the piezoelectric effect**

- **Non-Josephson emission via quasiparticle relaxation Superconducting cascade laser**